Atmos. Chem. Phys. Discuss., 15, 27253–27309, 2015
www.atmos-chem-phys-discuss.net/15/27253/2015/
doi:10.5194/acpd-15-27253-2015

Atmospheric Chemistry and Physics Discussions

Baseline carbon monoxide and ozone in the northeast US over 2001–2010

Y. Zhou[1], H. Mao[1], K. Demerjian[2], C. Hogrefe[3], and J. Liu[4,5]

[1]Department of Chemistry, State University of New York College of Environmental Science and Forestry, Syracuse, NY 13210, USA
[2]Atmospheric Science Research Center, State University of New York at Albany, Albany, NY 12203, USA
[3]Emissions and Model Evaluation Branch, Atmospheric Modeling and Analysis Division, NERL, ORD, U.S. EPA, Research Triangle Park, NC 27711, USA
[4]School of Atmospheric Sciences, Nanjing University, Nanjing 210093, China
[5]Department of Geography and Program in Planning, University of Toronto, 100 St. George Street, Toronto, ON M5S 3G3, Canada

Received: 17 August 2015 – Accepted: 5 September 2015 – Published: 8 October 2015

Correspondence to: Y. Zhou (yzhou51@syr.edu)

Published by Copernicus Publications on behalf of the European Geosciences Union.

Abstract

Baseline carbon monoxide (CO) and ozone (O_3) were studied at seven rural sites in the northeast US during varying periods over 2001–2010. Interannual and seasonal variations of baseline CO and O_3 were examined for the effects of changes in anthropogenic emissions, stratospheric intrusion, transport pathways and O_3 photochemistry. Baseline CO generally exhibited decreasing trends at most sites, except at Castle Spring (CS), an elevated (~ 400 m a.s.l.) site in rural central New Hampshire. Over April 2001–December 2010, baseline CO at Thompson Farm (TF), Pinnacle State Park (PSP), and Whiteface Mountain (WFM) decreased at rates ranging from −4.3 to −2.5 ppbv yr^{-1}. Baseline CO decreased significantly at a rate of −2.3 ppbv yr^{-1} at Mt. Washington (MWO) over April 2001–March 2009, and −3.5 ppbv yr^{-1} at Pack Monadnock (PM) over July 2004–October 2010. Unlike baseline CO, baseline O_3 did not display a significant long term trend at any of the sites, resulting probably from opposite trends in NO_x emissions worldwide and possibly from the overall relatively constant mixing ratios of CH_4 in the 2000s. In looking into long term trends by season, wintertime baseline CO at MWO and WFM, the highest sites, did not exhibit a significant trend, probably due to the competing effects of decreasing CO emissions in the US and increasing emissions in Asia. Springtime and wintertime baseline O_3 at TF increased significantly at a rate of 2.4 and 2.7 ppbv yr^{-1}, respectively, which was likely linked to nitrogen oxides (NO_x) emissions reductions over urban areas and possible resultant increases in O_3 due to less titration by NO in urban plumes. The effects of meteorology on baseline O_3 and CO were investigated. A negative correlation was found between springtime baseline O_3 and the North Atlantic oscillation (NAO) index. It was found that during positive NAO years, lower baseline O_3 in the northeast US was linked to less solar radiation flux, weakened stratospheric intrusion, and intensified continental export. The lowest baseline CO at Appledore Island (AI), PM, TF, PSP, WFM and the lowest baseline O_3 at AI, PM, and PSP in summer 2009 were linked to the negative phase of the Arctic oscillation (AO), when more frequent cyclone activities brought more clean Arctic air

to midlatitudes. It was also found that forest fires played a major role in determining baseline CO in the northeast US In summer, ∼ 38 % of baseline CO variability at AI, CS, MWO, TF, PSP, and WFM could be explained by CO emissions from forest fires in Russia and ∼ 22 % by emissions from forest fires in Canada. Long-range transport of O_3 and its precursors from biomass burning contributed to the highest baseline O_3 in summer 2003 at AI, CS, MWO, TF, and WFM. The findings of this study suggested impacts of increasing Asian emissions, NO_x emissions from the Northeast Urban corridor, global biomass burning emissions, and meteorological conditions (e.g. cyclone activity, AO, and NAO) should all be considered when designing strategies for meeting and maintaining National Ambient Air Quality Standards (NAAQS) and evaluating the air quality in the northeast US.

1 Introduction

Tropospheric ozone (O_3), which is produced largely by photochemical oxidation of nitrogen oxides (NO_x) and volatile organic compounds (VOCs), is a serious and ubiquitous air pollutant affecting humans' respiratory system, reducing yields of agricultural crops, and damaging natural ecosystems (EPA, 2012). As a precursor of hydroxyl radicals (OH), a dominant oxidant, O_3 regulates the atmospheric capacity of oxidation (Prinn, 2003). Tropospheric O_3 is also the third strongest greenhouse gas, after carbon dioxide (CO_2) and methane (CH_4), suggested by the Intergovernmental Panel on Climate Change (IPCC, 2007).

CO is a product of incomplete combustion (e.g. fossil fuel, biofuel, and biomass burning) and oxidation of hydrocarbon compounds (Worden et al., 2013). CO is a major sink of OH, and hence changes in CO can impact many chemically important trace species that are removed via oxidation by OH (Daniel and Solomon, 1998; Petrenko et al., 2013). In the presence of NO_x, CO oxidation is important in the tropospheric O_3 budget. Due to its relatively unreactive chemical nature, CO has been used as a tracer

of anthropogenic influence and fire emissions (Gratz et al., 2014; Price et al., 2004; Weiss-Penzias et al., 2006).

The United States has made enormous efforts to control ambient mixing ratios of criteria pollutants since the 1970s (EPA, 2012). Nationally, annual second maximum 8 h average mixing ratios of CO decreased by 52 %, and annual mean mixing ratios of nitrogen dioxide (NO_2) declined by 33 % over 2001–2010 (EPA, 2012). Ambient O_3 concentrations in metropolitan areas, such as Los Angeles, New York City, and Chicago, decreased significantly in the past two decades (Bell et al., 2007; Cooper et al., 2010, 2012; Lefohn et al., 2010; Parrish et al., 2011). Despite the decreasing anthropogenic emissions in Europe and North America, emissions in China and India have increased. Biomass burning emissions vary both spatially and temporally (Granier et al., 2011; Gratz et al., 2014). It remains unclear how such opposing changes in emissions have globally affected baseline CO and O_3, which are defined as mixing ratios of CO and O_3 under minimal influence of recent and local emissions (Chan and Vet, 2010; HTAP, 2010). Quantitative estimates of baseline CO and O_3 are not straightforward since measurements at a particular location include contributions from local anthropogenic precursor emissions (Chan and Vet, 2010). In the literature, air masses with low percentile values (< 20th percentile in the literature) of CO, an excellent anthropogenic tracer for its origin of mobile combustion, are commonly considered background air (e.g., Lin et al., 2000; Mao and Talbot, 2012). The low percentile value of CO is used as baseline CO, and baseline O_3 is then estimated using the data corresponding to CO mixing ratios below the baseline CO level (e.g., Lin et al., 2000; Mao and Talbot, 2012).

The lifetime of CO and O_3 in the free troposphere is ∼ 2 months and ∼ 20 days, respectively (Price et al., 2004; Stevenson et al., 2006). Thus, CO, O_3, and other precursors emitted in the upwind region and those produced in transit could be transported downwind and subsequently affect the baseline CO and O_3 levels there (Cooper et al., 2012; Oltmans et al., 2008; Pollack et al., 2013). This has important regulatory implications, because the levels of baseline CO and O_3 directly affect emission control of CO and other O_3 precursors. Therefore, quantifying trends and variations in baseline

CO and O_3 is of vital importance to assessing air quality and designing cost-effective emission control plans to meet the National Ambient Air Quality Standards (NAAQS) (http://www3.epa.gov/ttn/naaqs/criteria.html).

Studies have been conducted to investigate trends in baseline CO and O_3 across northern hemispheric mid-latitudes, such as North America, Europe, and Asia (Chan, 2009; Cooper et al., 2010; Cui et al., 2011; Logan et al., 2012; Oltmans et al., 2013; Parrish et al., 2012; Tilmes et al., 2012; Wilson et al., 2012; Xu et al., 2008). No consistent trends have been found. Kumar et al. (2013) reported trends of −0.31 and −0.21 ppbv yr^{-1} for CO and O_3, respectively, at the Pico Mountain Observatory over 2001–2011. Gratz et al. (2014) reported that the springtime median mixing ratio of O_3 increased at a rate of 0.76 ppbv yr^{-1} at the Mt. Bachelor Observatory over 2004–2013, while median CO decreased at a rate of −3.1 ppbv yr^{-1}. Chan and Vet (2010) found that baseline O_3 in the eastern US decreased in spring, summer, and fall over 1997–2006, and the decadal trends in the Atlantic coastal region were positive in winter, summer, and fall. For the most part, causes for temporal variability have not been adequately explained. Interpretation of long-term trends is difficult because of significant interannual variability in emissions and climate as well as possibly in photochemistry (Hess and Lamarque, 2007). Climate change may lead to changes in natural emissions (e.g., emissions from wildfires, vegetation, and lightning), pollution transport pathways, and stratosphere-tropospheric exchange (Parrish et al., 2013).

Wildfires release large quantities of O_3 precursors, e.g., CO, VOCs, and NO_x, every year. For instance, the MACCity emission inventory over 2001–2010 suggested that total global biomass burning emissions of CO ranged from ∼ 300 to ∼ 460 Tg yr^{-1}, close to ∼ 590 Tg yr^{-1} anthropogenic emissions (Granier et al., 2011). These chemical species could make a significant contribution to tropospheric CO and O_3 budgets, impacting the interannual variability of surface CO and O_3 globally (Dutkiewicz et al., 2011; Herron-Thorpe et al., 2014; Honrath et al., 2004; Kang et al., 2014; Wigder et al., 2013; Wotawa and Trainer, 2000). Most studies demonstrated elevated CO and O_3 due to fire emissions for an episode (Dutkiewicz et al., 2011; Honrath et al., 2004). To the

best of our knowledge, only two studies (Jaffe et al., 2004; Wotawa et al., 2001) quantified the impact of wildfires on baseline CO and O_3 in the 1990s using ten-year observations. More research is warranted to determine the impact of wildfires on baseline CO and O_3 in the 2000s in northern hemispheric midlatitudes.

Regional climatic processes over the US east coast are influenced by the North Atlantic Oscillation (NAO) and the Arctic Oscillation (AO) (Archambault et al., 2008; Hess and Lamarque, 2007). Studies suggested a link between NAO and regional distributions of tropospheric trace gases over the northwestern Atlantic Ocean, northern Europe, and the Arctic region based on model simulations or measurements (Christoudias et al., 2012; Creilson et al., 2003; Duncan and Bey, 2004; Eckhardt et al., 2003; Hegarty et al., 2009; Krichak and Alpert, 2005; Li et al., 2002; Pausata et al., 2012; Woollings and Blackburn, 2012). Most studies suggested that trace gases over North America could be transported across the Atlantic Ocean to northern Europe during the high NAO phase, particularly in winter and spring. However, to the best of our knowledge, nearly no studies examined the relationship between NAO and trace gases over the northeast US Circulation patterns can not only impact the transport of pollutants to the targeted region but can also influence the export from the upwind region. Hence, upwind trace gases are also likely to change in response to varying intensity of NAO.

The AO is another dominant mode of meteorological variability in the Northern Hemisphere (Creilson et al., 2005; Hess and Lamarque, 2007; Pausata et al., 2012). AO is characterized by winds circulating counterclockwise around the Arctic at around 55° N latitude, (Thompson and Wallace, 2000). In a positive AO phase, surface pressure in the polar region is abnormally low and strong winds around the pole confine cold air masses in the Arctic region; otherwise, more Arctic cold air dives south and increases storminess in the mid-latitudes (Thompson and Wallace, 2000). Oswald et al. (2015) hypothesized that observed higher summertime O_3 levels in the northeast US was associated less storminess in a positive AO phase. Some modeling studies suggested a weak impact from stratosphere-tropospheric exchange of O_3 on the lower tropo-

sphere over the Atlantic basin during a positive AO year (Brand et al., 2008; Hess and Lamarque, 2007; Lamarque and Hess, 2004). The impact of AO on surface O_3 in the northeast US needs to be further investigated using long-term surface measurement data.

Our study used long-term observations at seven rural sites in the Northeast US Five are located in rural New Hampshire (NH) and two are in rural New York (NY) State. Although numerous studies have been conducted to understand the distributions of surface CO and O_3 in the northeast US and their controlling mechanisms (e.g. Bae et al., 2011; Hegarty et al., 2009; Lai et al., 2012; Mao and Talbot, 2004; Schwab et al., 2009; Zhou et al., 2007), little work was done on baseline CO and O_3 using long-term measurement data for the region. Here, the trends of baseline CO and O_3 were examined at each site for the time period of 2001–2010, and regional to global emissions and large scale circulation patterns were investigated for their roles in the interannual and seasonal variation of baseline CO and O_3.

2 Methods and data

2.1 Measurement data

The seven rural sites selected in this study (Table 1 and Fig. 1) are within a few hundred kilometers of each other. Their elevation varies between 18 and 2100 m. Measurements of CO, O_3, wind direction, wind speed, and relative humidity at Appledore Island (AI), Castle Spring (CS), Mount Washington (MWO), Pack Monadnock (PM), and Thompson Farm (TF) were conducted by the University of New Hampshire (UNH) AIRMAP Observing Network (http://www.eos.unh.edu/observatories/data.shtml). The time resolution of the continuous year-round measurements at these five sites was one minute. At AI, CO was measured seasonally from May to September over 2001–2006 and year-round over 2007–2011, and O_3 was measured seasonally from May to September over 2002–2007 and year-round over 2008–2011. The description of CO and O_3 measure-

ment techniques from the UNH AIRMAP sites can be found in Mao and Talbot (2004). Additionally, hourly data of solar radiation flux were available at TF over January 2002–December 2010 from the Climate Reference Network (CRN) run by the National Ocean and Atmospheric Administration (NOAA) (http://www.ncdc.noaa.gov/data-access). The one-hour measurement data of CO, O_3, wind direction, wind speed, and relative humidity at Whiteface Mountain (WFM) and Pinnacle State Park (PSP) began around 1996 (Table 1). The description of CO and O_3 measurement techniques for WFM and PSP can be found in Brandt et al. (2015) and Schwab et al. (2009). The time in all of the datasets was expressed in coordinated universal time (UTC), i.e. local time +5 h for non-daylight saving time and +4 h for daylight saving time (March–November).

2.2 Quantification of baseline CO and O_3

The local afternoon time window (18:00–24:00 UTC) was selected to avoid including the data representing nighttime depletion of O_3 due to dry deposition and titration (Talbot et al., 2005). The planetary boundary layer (PBL) is well mixed in the afternoon. The monthly 10th percentile mixing ratio of CO at AI, CS, PM, TF, and PSP was used to represent the baseline CO levels. As MWO and WFM are located atop the mountains, they are far less impacted by local anthropogenic emissions. Therefore, monthly median values of CO were selected at MWO and WFM to represent the baseline level. To determine baseline O_3 levels, we first created a subset of O_3 data by using the O_3 mixing ratios corresponding to CO mixing ratios below the monthly 10th percentile values at AI, CS, PM, TF, and PSP and monthly median values at MWO and WFM. The monthly median values of this subset were then defined as the baseline O_3 levels for respective sites.

2.3 Datasets

The NAO index is a measure of the intensity of NAO, which is defined based on the leading empirical orthogonal function of the normalized sea level pressure difference

between the subtropical high and the subpolar low using the National Centers for Environmental Prediction/National Center for Atmospheric Research (NCEP/NCAR) reanalysis (Barnston and Livezey, 1987). The AO index was obtained by projecting the daily 1000 hPa geopotential height anomalies poleward of 20° N onto the loading pattern of the AO (Thompson and Wallace, 2000). The Climate Prediction Center of NCEP (http://www.cpc.ncep.noaa.gov/data/teledoc/telecontents.shtml) routinely monitors the primary teleconnection patterns. Monthly climate index values of NAO and AO were used in this study to understand the roles of global transport of atmospheric species via large-scale atmospheric circulation.

The Global Fire Emission Data (GFED) combines satellite information of fire activities and vegetation productivities, and contains the gridded monthly burned area and fire emissions. GFED 3 (http://www.globalfiredata.org/) was used in this study to estimate the biomass burning emissions of CO over Russia, Canada, California, and Alaska. Data were available for 2001–2010 at 0.5° × 0.5° horizontal resolution. Monthly mean global CO columns with 1° × 1° resolution obtained from the Measurements of Pollution in the Troposphere (MOPITT) instrument on the satellite Terra (https://www2.acd.ucar.edu/mopitt/) were used for the time period of 2001–2010 over grids containing Russia, Canada, Alaska, and California, when wildfire CO emissions in these grids calculated from GFED were larger than 1 g m^{-2} month^{-1}.

Monthly wind, geopotential height, temperature, relative humidity (http://www.esrl.noaa.gov/psd/data/gridded/data.ncep.reanalysis.html), potential vorticity (PV) (http://rda.ucar.edu/datasets/ds090.0) with a spatial resolution of 2.5° × 2.5° from the NCEP/NCAR Global Reanalysis Products were used for meteorological conditions and for identifying stratospheric intrusion.

The dataset representing O_3 of stratospheric origin, constructed by Liu et al. (2013) (ftp://es-ee.tor.ec.gc.ca/pub/ftpdt/Stratospheric%20Climatology/), was also used to verify the contribution of stratospheric O_3 to the two mountain sites and the decadal trends there. This dataset included monthly amounts of stratospheric O_3 from the surface to 26 km altitude with 5° × 5° × 1 km spatial resolution from the 1960s to the 2000s.

Mean sea level pressure data were obtained from NCEP-DOE Reanalysis 2 (http://www.esrl.noaa.gov/psd/data/gridded/data.ncep.reanalysis2.html). The dataset is six hourly with a spatial resolution of 2.5° × 2.5°. The data were used to identify and quantify the cyclones that passed over the northeast US.

2.4 Mid-latitude cyclone identification and tracking

Many algorithms have been developed since the 1970s to identify mid-latitude cyclones (Hu et al., 2004; Murazaki and Hess, 2006; Racherla and Adams, 2008). The algorithm developed by Bauer and Del Genio (2006) was adopted in this study to track the sea level pressure minima. The first step of the algorithm was to search for the local minimum by a 2 grids × 2 grids matrix. The next step was to search for the local (within 720 km) minimum in the next 6 h time step, assuming that a cyclone cannot move faster than 120 km h^{-1}, the same criterion used by Bauer and Del Genio (2006). If more than one local minimum was found, the center of a cyclone was obtained. Two more criteria were applied, its duration > 24 h and central pressure ≤ 1020 hPa. Long-term cyclone frequency statistics were calculated for the northeast US (37.5–47.5° N, 67.5–82.5° W).

2.5 Statistical methods

The open-air package in the statistical programming language R 3.0.2 was used to determine whether a rate of change was statistically significant. Trends in baseline CO and O_3 were reported using SenTheil slopes from the non-parametric Mann–Kendall analysis in ppbv yr^{-1} with 90 % confidence intervals. Pearson correlation was computed to determine the relation between variables (e.g. baseline CO, baseline O_3, NAO index, relative humidity). The Student t test was conducted to verify statistical significance ($\alpha = 0.10$).

To quantify the contribution to a location of interest from biomass burning emissions over an area, we applied the following linear regression models (Wotawa et al., 2001):

$$CO = a_0 + a_1 E \quad (1)$$

Where CO is the mixing ratio of baseline CO at each site, E the total CO column over the area, a_0 the intercept value, and a_1 the slope value. The combined effect of biomass burning emissions from Russia (E_{Russia}) and Canada (E_{Canada}) was computed using Eq. (2):

$$\text{CO} = b_0 + b_1 E_{\text{Russia}} + b_2 E_{\text{Canada}} \quad (2)$$

where b_0, b_1, and b_2 are regression parameters. Note that E_{Russia} and E_{Canada} were found to be the two emissions sources that contributed significantly to the baseline CO at the seven sites of our study, which is why only these two sources were included in the regression.

3 Results and discussions

3.1 General characteristics

3.1.1 Baseline CO

Baseline CO at CS, MWO, PM, TF, and PSP had maxima uniformly in March and minima in varying months over August–October (Fig. 2a and b). Averaged annual maxima were 191 ppbv at CS, 180 ppbv at MWO, 155 ppbv at PM, 164 ppbv at TF, and 189 ppbv at PSP over their respective time periods (Table 1). Averaged annual minima were 131 ppbv in August at CS, 142 ppbv in September at MWO, 109 ppbv in October at PM, 113 ppbv in August at TF, and 128 ppbv in October at PSP. At AI, year-round data were available during 2007–2010, a much shorter time period compared to those at other sites. The seasonal cycles at AI were consistent with other sites, with the average annual maximum 149 ppbv in March and minimum 103 ppbv in September. Previous studies suggested that the annual maximum in cold months resulted from residential heating, vehicle cold starts, and less loss from oxidation by OH, while the annual minimum in fall, instead of in June–July when solar radiation and hence OH concentrations

reach annual maxima, was probably the combined effect of biomass burning emissions, mobile combustion emissions, and loss from oxidation by OH (Kopacz et al., 2010; Miller et al., 2008).

The annual cycle at WFM was different from those at all other sites, with an annual maximum of 144 ppbv in July and minimum of 103 ppbv in December averaged over January 2001–December 2010 (Fig. 2b). To investigate the potential reasons for this different behavior, the data at WFM were compared with those at MWO, a site with slightly higher elevation (2 km a.s.l.) located 208 km to the east (Fig. 1). WFM and MWO are 128 km southwest and 217 km southeast, respectively, from Montreal, the 9th largest city in North America. Over 2001–2009, averaged summertime baseline CO (141 ppbv) at WFM was comparable to that (145 ppbv) at MWO, while averaged wintertime baseline CO (108 ppbv) at WFM was 60 ppbv or 36 % less than that (168 ppbv) at MWO (Fig. 2a and b). This wintertime contrast was probably associated with the large difference between the frequency distributions of wind direction at the two sites. There were 4.7 % of the air masses at WFM from the northeast (22.5–67.5°), compared to 75.4 % of the air masses at MWO from the northwest (247.5–337.5°), the general direction of Montreal. This indicates that MWO was frequently exposed to northwesterly winds carrying air masses potentially influenced by anthropogenic emissions in Montreal, while such influences were rare at WFM. Consequently, much lower baseline CO was found at WFM than at MWO.

From April 2001 to December 2010, baseline CO decreased significantly at a rate of $-2.5\,\text{ppbv}\,\text{yr}^{-1}$ at TF, $-4.3\,\text{ppbv}\,\text{yr}^{-1}$ at PSP, and $-2.8\,\text{ppbv}\,\text{yr}^{-1}$ at WFM. Baseline CO decreased at a rate of $-2.3\,\text{ppbv}\,\text{yr}^{-1}$ at MWO over April 2001–March 2009 and $-3.5\,\text{ppbv}\,\text{yr}^{-1}$ at PM over July 2004–October 2010 (Table 2). Unlike all other sites, CS exhibited an increasing trend of $2.8\,\text{ppbv}\,\text{yr}^{-1}$ over April 2001–June 2008. Prior to May 2003, the mixing ratio of baseline CO at CS was similar to that at TF. After May 2003, baseline CO at CS was ~ 30 ppbv higher than that at TF and PM (Fig. 2a), resulting in the overall increasing trend. The reasons for such unusually high values at CS are unknown.

The U.S. EPA reported a decrease of 52 % in the national average of annual second highest 8 h mixing ratios of CO from 2001 to 2010 (EPA, 2012), corresponding to a rate of $-7.8\,\mathrm{ppbv\,yr^{-1}}$ (for an decadal average mixing ratio of ~ 150 ppbv), which was larger than that at any of our sites. Because EPA's trend was estimated using measurements mainly from urban sites with higher concentrations and also focused on the high end of the distribution, it is expected to show larger changes compared to the trend of baseline levels at rural or remote sites from this study, with influence of direct anthropogenic emissions removed.

The total CO column from MOPITT retrievals over the eastern US was found to decrease at a rate of $1.4\,\%\,\mathrm{yr^{-1}}$ (or $-2.1\,\mathrm{ppbv\,yr^{-1}}$ for a decadal average mixing ratio of ~ 150 ppbv) from 2000 to 2011 (Worden et al., 2013), which was comparable to that of the baseline CO in this study. These significant decreasing trends of baseline CO and total column CO were probably associated in large part with anthropogenic CO emissions reductions worldwide (Gratz et al., 2014). Globally, anthropogenic CO emissions showed a slight decrease of ~ 1 % from 1990 to 2010 (Granier et al., 2011). In the US and Europe, total anthropogenic CO emissions declined at a rate of $-3\,\%\,\mathrm{yr^{-1}}$ from 2000 to 2010, while increasing trends were found in India ($\sim 1.5\,\%\,\mathrm{yr^{-1}}$) and China ($\sim 3\,\%\,\mathrm{yr^{-1}}$) (Granier et al., 2011). A decreasing trend in CO emissions in China since 2005 was suggested by Tohjima et al. (2014) and Zhang et al. (2009).

3.1.2 Baseline O_3

The baseline O_3 concentrations from all sties ranged from 22 ppbv in the fall to 56 ppbv in spring, consistent with baseline levels in the Eastern US that were quantified using a principal component analysis and backward air parcel trajectories by Chan and Vet (2010). The time series of baseline O_3 at all sites showed averaged annual maxima in April and minima in August–October (Fig. 2c and d). Annual maxima averaged over their respective periods at the seven sites occurred all in April and were very close in magnitude, ranging from 47 to 51 ppbv. In comparison, averaged annual minima at the seven sites displayed distinct difference in magnitude and timing, varying over 28–

37 ppbv, occurring in August at CS, September at AI and PM, and October at TF, PSP, MWO, and WFM. Studies have suggested that monthly surface O_3 over remote continental areas generally had a spring maximum, attributed to enhanced stratospheric input and hemispheric wide photochemical production (Monks, 2000; Parrish et al., 2013). Here, the fact that baseline CO had annual maxima in spring suggested that the springtime annual maxima of baseline O_3 were possibly associated with photochemical processing of O_3 precursors including CO and VOCs that had been built up over winter on a hemispherical scale (Kopacz et al., 2010; Penkett et al., 1993).

A close examination using the Mann–Kendall test suggested no significant trends in baseline O_3 during the study period at all sites (Table 2). Similar results were found in Mace head, Ireland, which is located on the western coast of Europe (Derwent et al., 2007). From 1987 to 1997, baseline O_3 at Mace Head had a significant increasing trend of $0.14\,\mathrm{ppbv\,yr^{-1}}$ followed by a small increase over 1997–1999, and stabilized over 2000–2007 (Derwent et al., 2007).

IPCC (2001) suggested that the change of long-term trends in baseline O_3 could be driven by CH_4 oxidation in the presence of NO_x. In a polluted region, O_3 is produced by photochemical reactions of nonmethane hydrocarbons (NMHCs) and NO_x (West et al., 2006). In the global troposphere, CH_4 is the primary anthropogenic VOC (Fiore et al., 2002) and affects global background mixing ratios of O_3 due to its long lifetime (8–9 years). Derwent et al. (2007) found the change of baseline O_3 in Mace Head followed the mixing ratios of baseline CH_4 over 1992–2007. West et al. (2006) found that reducing global anthropogenic CH_4 emissions by 20 % beginning in 2010 would reduce O_3 mixing ratios globally by ~ 1 ppbv in 2030. Globally, the growth rate of CH_4 declined from $\sim 13\,\mathrm{ppbv\,yr^{-1}}$ in the early 1980s to near zero over 1999–2006 (WMO, 2012). Since 2007, atmospheric CH_4 was increasing again with an average rate of $\sim 3\,\mathrm{ppbv\,yr^{-1}}$ (WMO, 2012). These changes in CH_4 mixing ratios can potentially lead to changes in baseline O_3 mixing ratios.

On the other hand, global NO_x emissions did not change overall during the study period (Granier et al., 2011). Granier et al. (2011) reported that annual NO_x emissions

decreased at a rate of 1.5 Tg yr^{-1} in western Europe, 0.7 Tg yr^{-1} in central Europe, ~ 5 Tg yr^{-1} in the US over 2001–2010, while increased at a rate of ~ 5 Tg yr^{-1} in China and ~ 1.5 Tg yr^{-1} in India. Xing et al. (2015) found varying trends in NO_x mixing ratios over 1990–2010, with 4.1 % in China, −1.4 % in the US, and −1.2 % in Europe. The annual rates of change in NO_x concentrations were comparable to those in emissions (Xing et al., 2015). This suggests that increasing CH_4 and opposite trends of NO_x emissions worldwide probably contributed to the insignificant trends in baseline O_3 over the northeast US during 2001–2010.

3.2 Seasonal variation of decadal trends in baseline CO and O_3

Generally a decreasing trend was found in baseline CO and no trend in baseline O_3 during the decade 2001–2010 as shown in the previous section. However, trends of baseline CO and O_3 were found to vary by season (Table 2). Baseline CO at CS was anomalously high since May 2003 (Fig. 2a) and had increased over the decade in all seasons. As the reasons for the unusually high values at CS are unknown, baseline CO at CS was not included in the subsequent discussion.

In spring and winter, baseline CO at PM, TF, and PSP decreased significantly at a rate between −6.5 to −3.7 ppbv yr^{-1}, while no significant decreasing trends were found at the two highest sites MWO and WFM (Table 2). In summer, baseline CO at MWO, PM, TF, and PSP showed decreasing trends varying between −5.5 and −4.3 ppbv yr^{-1}. In fall, baseline CO at all sites decreased significantly at rates varying between −6.4 and −3.2 ppbv yr^{-1}.

The overall insignificant change of baseline CO at MWO and WFM in spring and winter could be due to the combined effect of decreasing US emissions and increasing Asian emissions. MWO and WFM are the highest sites situated close to the top of the daytime convective boundary layer, which are more likely impacted by free tropospheric air compared to other sites. Thus, the impact of continental to intercontinental transport could be just as important there, and perhaps at times more important, than regional

transport. CO emissions in the US declined at a rate of ~ −3 % yr^{-1} over 2000–2010, while an overall increasing trend was seen in China over 1999–2010, despite a small decrease since 2005 (Granier et al., 2011; Tohjima et al., 2014). Liang et al. (2004), using GEOS-Chem model simulations, found that Asian influence was strongest in spring in the North Pacific lower troposphere, due to the combined effect of efficient ventilation of the Asian boundary layer via midlatitudinal cyclones and convection, long lifetime of CO, and strong springtime biomass burning emissions in southeastern Asia. The same study also found that the Asian influence weakened in summer due to the shorter lifetime of CO and continental export driven most often by convective injection to the upper troposphere, while particularly strong transpacific transport events occurred in spring and winter (Liang et al., 2004).

In fall, baseline O_3 did not show significant trends at any of the sites (Table 2). In summer, baseline O_3 showed distinct decreasing trends of −3.1 ppbv yr^{-1} at AI, −4.7 ppbv yr^{-1} at both MWO and WFM during their respective time periods, and no trends were found at other sites (Table 2). TF was the only site where baseline O_3 increased significantly at a rate of 2.4 ppbv yr^{-1} in spring and 2.7 ppbv yr^{-1} in winter over 2001–2010, while other sites showed no trends during the two seasons.

Tropospheric O_3 has been changing over the past four decades in response to changes in anthropogenic and natural emissions, stratosphere-tropospheric exchange, pollution transport pathways and O_3 photochemistry (Parrish et al., 2013). Therefore, it was hypothesized that the following factors may have contributed to the significant decreasing trends in summertime baseline O_3 at AI, MWO, WFM and significant increasing trends in springtime and wintertime baseline O_3 at TF:

1. Decreasing and increasing stratospheric intrusion in summer and winter – spring, respectively;

2. Decreasing and increasing continental to intercontinental transport of anthropogenic and natural O_3 precursors in summer and winter – spring, respectively;

3. Decreasing emissions of NO_x from electric power generation and motor vehicles; and

4. Changing pollution transport pathways in winter, spring, and summer.

Factor #1 was examined using PV data, as one of the physical characteristics of stratospheric air is high value of PV. Time series of PV at 350 K showed no trend in PV over the northeast US during the decade (Fig. 3a). There appeared to be distinct annual cycles in PV with maxima in winter and minima in summer, averaged 1.81×10^{-8} and $1.05 \times 10^{-8}\,m^2\,s^{-1}$ kg, respectively (Fig. 3a). Hence, stratospheric intrusion probably had a larger impact on the surface in winter-spring than in summer, which was supported by previous studies (James et al., 2003; Stohl et al., 2003). Such impact would more likely reach higher than lower elevation locations. No trends in baseline O_3 at the two highest sites MWO and WFM appeared to be consistent with what the time series of PV suggested. Moreover, TF, near the sea level (18 m a.s.l.), was less likely influenced by stratospheric intrusion than all other sites. These points were verified using the stratospheric O_3 during 2001–2010 from Liu et al. (2013), which suggested, on seasonal average in the area including all our sites, no contribution to the lowest layer (0.5 km) in summer, or no significant trends in such contribution in winter-spring. Therefore, it seemed unlikely that stratospheric intrusion contributed to the springtime and wintertime increasing trends in baseline O_3 at TF.

Significant increases have been reported by Cooper et al. (2012) in springtime and wintertime free tropospheric O_3 over North America, particularly in air masses originating from East Asia. The western US with elevated terrain was much more likely to be influenced by descending free tropospheric air than the eastern US (Cooper et al., 2012). Even if air masses rich in O_3 originating from East Asia reached the US East Coast, they would most likely have a stronger impact on elevated sites. The fact of no trends at any of the elevated sites in spring or winter suggested that long-range transport of O_3 and its precursors from Asia was probably not a cause of increasing springtime and wintertime baseline O_3 at TF (Factor #2).

In summer, continental export from East Asia is weaker (Wild and Akimoto, 2001) and Asian emissions have less impact on US surface O_3 relative to domestic emissions than in winter and spring (Reidmiller et al., 2009), which ruled out the effect of long-range transport of Asian emissions on summertime trends in baseline O_3 at our sites. Summer sees the peak of forest fires (Wotawa et al., 2001). Therefore, changes in emissions of CO and other O_3 precursors from biomass burning could influence the trends in summertime baseline O_3 and CO (Sect. 3.3.1).

Further analysis suggested that decreasing urban emissions of NO_x quite likely contributed to the rise in springtime and wintertime baseline O_3 at TF (Factor #3). Tropospheric NO_2 column over the US declined by 41 % in spring and 33 % in summer during the period of 1996–2011 (Cooper et al., 2012). Emissions of NO_x in the US were reduced by 48 % over 1990–2010, largely due to control of emissions from power plants and mobile sources (Xing et al., 2013). The Northeast US Urban Corridor, extending from Washington D.C. in the south to Boston in the north, was dominated by mobile combustion emissions of NO_x. Annual mixing ratios of NO_2 in New York City decreased at a rate of $-0.3\,ppbv\,yr^{-1}$ over 1980–2007 (Buckley and Mitchell, 2011). In winter and early spring with weakened photochemical production, decreased NO_x emissions in urban areas could cause less loss of O_3 via titration by NO (Liu et al., 1987; Jacob et al., 1995; Frost et al., 2006; Jonson et al., 2006), and the result could be enhanced O_3 mixing ratios in urban plumes (Cooper et al., 2010; Wilson et al., 2012). From measurements at our sites, data points of O_3 were selected corresponding to wind from the urban corridor. It was found that the 10th percentile mixing ratio of O_3 at TF in air masses from the urban corridor had been increasing at a rate of $1.81\,ppbv\,yr^{-1}$ ($p = 0.05$) in spring and $1.52\,ppbv\,yr^{-1}$ ($p < 0.01$) in winter (Fig. 3b and c). This strongly suggests that decreased NO_x emissions in the urban corridor likely had a significant impact on springtime and wintertime baseline O_3 at TF whereas had no similar effects at other sites. In summer with strong photochemistry, decreased emissions of O_3 precursors could lead to reductions in peak summertime O_3 concentrations at surface continental sites (Cooper et al., 2012; Parrish et al., 2013). No significant change was

found in summertime 10th percentile mixing ratios of O_3 in air masses from the urban corridor at TF, which was consistent with the relatively constant summertime baseline O_3 at TF as aforementioned.

The implementation of the Acid Rain Program and the NO_x Budget Trading Program (NBP) also reduced NO_x emissions from the power plants (Xing et al., 2013). In the Ohio River Valley, where power plants dominate, both NO_2 column and NO_x emissions decreased by 38 and 34 % over 1999–2005 (Kim et al., 2006). However, the 10th percentile mixing ratio of O_3 in air masses from the southwest did not show any significant change in winter, spring, and summer at PSP, which is located to the northeast of the Ohio River Valley (Fig. 3b–d).

There is interannual variability in transport pathways, temperature, water vapor, solar radiation, and natural emissions (e.g., lightning, forestfires, and vegetation). A close examination of the NOAA CRN data revealed that springtime solar radiation at TF was increasing at a rate of $24.5\,W\,m^{-2}\,yr^{-1}$ ($p = 0.03$) over 2002–2010, with the lowest value of $432\,W\,m^{-2}$ in 2002 (Fig. 3a), while no significant trend was found in winter. Without the value in spring 2002, the solar radiation flux at TF increased at a rate of $9.4\,W\,m^{-2}\,yr^{-1}$ in spring ($p = 0.02$). This trend in springtime solar radiation at TF was possibly related to cloudiness in response to changing cyclone activity associated with varying atmospheric circulation, which could have affected baseline O_3. The impact of changes in weather conditions and large scale circulation on baseline O_3 was further explored in the following section.

3.3 Factors controlling baseline CO and O_3 in spring and summer

This section further identifies factors impacting the variation of baseline CO and O_3. Emphasis was placed on spring and summer, when there are strong intercontinental transport and photochemistry involving O_3 and CO (Cooper et al., 2010; Emmons et al., 2003), as well as exceedances of NAAQS.

3.3.1 Impact of wildfires in summer

Large interannual variability in global CO mixing ratios was attributed to variations in biomass burning emissions (Novelli et al., 2003; Wotawa et al., 2001). Studies (Hecobian et al., 2011; Oltmans et al., 2010) suggested that biomass burning effluents from Russia and Canada flowed into North America. In addition, California and Alaska were two US states with considerable fire emissions of CO, which reportedly impacted the air quality over North America (McKendry et al., 2011; Real et al., 2007).

Fire emissions of CO in summer were estimated using the GFED dataset and MOPITT retrievals (Fig. 4a and b). The GFED data suggested that massive wildfires occurred in Russia in 2002, 2003, and 2008 with annual CO emissions of 42.1, 71.1, and 35.8 Tg, respectively. Annual fire emissions from Canada were 17.4 Tg in 2004 and 18.3 Tg in 2010. In Alaska, the largest fires occurred in 2004 with 13.1 Tg CO emitted, while in California the largest fire emissions of CO were 1.3 Tg in 2008. From 2001 to 2010, the total CO emissions from wildfires in Russia, Canada, Alaska and California varied from 19.9 to 84.3 Tg, with the lowest and the highest in 2007 and 2003, respectively.

To quantify contributions of wildfires from these four areas to summertime baseline CO levels at our sites, a linear regression model was used together with MOPITT total CO column retrievals. Monthly CO columns were first correlated with monthly GFED fire emissions of CO for the four areas. The correlation coefficients were 0.89, 0.81, 0.81, and 0.84 ($p < 0.01$ for the four values) for Russia, Canada, California, and Alaska, respectively, suggesting that the variability in total column CO over those areas was dominated by that of fire emissions.

Further, it was found that the contributions of fire emissions from Russia and Canada to the variability of summertime baseline CO at the 6 sites were averaged to be 38 and 22 %, respectively (Table 3), and their combined contribution was averaged to be 41 %. Contributions from Alaska and California were negligible at these six sites. Globally, there is approximately 1 billion ha closed forest in the boreal region, about two thirds of

which is situated in Russia (Harden et al., 2000). CO emissions from wildfires in Russia and Canada contributed 49.5 and 29.6 %, respectively, to the total CO emissions from wildfires in Northern Hemispheric midlatitudes (30–90° N). Understandably, baseline CO was well correlated to wildfires in Russia and Canada at most sites except at PSP.

The insignificant correlation between baseline CO at PSP and wildfires emissions from Russia and Canada was possibly due to less dynamical circulation at the site. PSP had the lowest wind speed of 0.47 m s^{-1} amongst all sites based on surface wind speed averaged over summers of 2001–2010 (Fig. 5a). This appeared to be consistent with the position of PSP relative to the pressure systems throughout the year (Fig. 5b–e). The climatological seasonal maps of sea level pressure suggest that PSP is located either on the periphery of the subtropical high in summer – fall, or the periphery of the North American trough, where wind tends to be the weakest. In comparison, other sites are either located at the top of the boundary layer, and/or tend to be positioned within the North American trough, more directly under the influence of the westerly wind often facilitating global transport.

Since wildfires provide a substantial source of NO_x and hydrocarbons, O_3 is expected to form in fire plumes. Some of these air pollutants live long enough to travel over long distances, which could elevate baseline O_3 globally (Jaffe et al., 2004). Corresponding to the largest fire emissions in summer 2003 in Russia (Fig. 4a), baseline CO in that season at all sites reached the decadal maxima, and baseline O_3 was the highest of all summers at AI, CS, MWO, TF, and WFM (Fig. 4c and d). Jaffe et al. (2004) also suggested that emissions from Siberia forest fires in summer 2003 were transported to North America resulting in enhancements of 23–37 and 5–9 ppbv in summertime baseline CO and O_3, respectively, at 10 sites in Alaska, Canada, and the Pacific Northwest.

The second largest summertime baseline CO mixing ratio of the decade was found in summer 2004 at CS, TF, and WFM (Fig. 4c), although the total CO emissions from wildfires in Russia and Canada during that season was 20.4 Tg, 16 % smaller than 24.4 Tg, the decadal (2001–2010) average annual CO emissions from the two countries. Over Alaska, the geopotential height in summer 2004 was ~ 40 gpm higher than

normal years (Fig. 6a–c). This relatively higher pressure field led to drier and warmer conditions over Alaska and southwestern Canada with 82 % relative humidity and 12 °C surface temperature, the driest and warmest of the decade (Fig. 6d). Such weather conditions are conducive to occurrence of wildfires. In summer 2004, CO emissions from wildfires in Canada and Alaska contributed 48.5 and 36.5 %, respectively, to the Northern Hemispheric total, compared to the decadal (2001–2010) average contributions of 49.5, 10.6, and 29.6 % from Russia, Alaska, and Canada, respectively. Correspondingly, the 13.1 Tg CO emissions from wildfires in Alaska were the largest over the decade, and the 17.4 Tg CO emissions from wildfires in Canada were the second largest of the decade, following the largest in summer 2010 (Fig. 4a). On the other hand, the streamlines over Canada suggested an unusually strong northeasterly component in summer 2004. The high pressure system over Alaska and southwestern Canada most likely strengthened the westward transport of wildfires effluents from Alaska and Canada (Fig. 6c). The combination of these two factors resulted in efficient transport of massive CO emissions from fires over Alaska and Canada. Smoke from these fires over the continental United States was observed in satellite images of aerosol optical depth (AOD) from the GOES (Geostationary Operational Environmental Satellites) (Kondragunta et al., 2008) and MODIS (Moderate Resolution Imaging Spectro-radiometer) aboard Terra (Mathur, 2008), and extensive plumes of enhanced CO concentrations were captured in MOPITT (Measurements of Pollutants in the Troposphere) retrievals (Pfister et al., 2005).

Mann–Kendall trend analysis indicated no significant decreasing trends in biomass burning emissions from Alaska, Canada, and California. In contrast, CO emissions from wildfires in Russia decreased at a rate of −0.51 Tg yr^{-1} (p = 0.10). Summertime baseline CO at MWO, PM, TF, and PSP decreased at a rate between −5.5 and −4.3 ppbv yr^{-1} and baseline O_3 at AI, MWO, and WFM decreased at a rate between −4.7 and −3.1 ppbv yr^{-1} (Sect. 3.2). Based on regression analysis, as a result of a 0.51 Tg yr^{-1} decrease in CO emissions from wildfires in Russia, baseline O_3 decreased by 0.04–0.07 ppbv yr^{-1} (p = 0.08–0.10) at AI, MWO, WFM, and CS, while

baseline CO declined by 0.14–0.22 ppbv yr^{-1} (p = 0.01–0.10) at AI, TF, MWO, and WFM. Hence, the decreasing trend of biomass burning emissions in Russia was likely a major factor causing the decreasing trends in baseline CO and O_3 in summer at our sites.

3.3.2 Impact of cyclone activity and AO in summer

Meteorology is another factor that can influence summertime baseline CO and O_3 across the northeast US of all the meteorological variables, midlatitude cyclone frequency is an important one that can impact regional air quality greatly. It affects not only boundary layer ventilation, humidity, solar radiation, and temperature but also general circulation of the regional atmosphere (Leibensperger et al., 2008).

Time series of summertime counts of cyclones in the northeast US showed strong interannual variability (Fig. 7a). The counts of cyclones in 2003, 2006, 2008, 2009, and 2010 were greater than 12, the average of summer 2001–2010. Summer 2009 experienced the largest number of cyclones (20) passing the northeast US during the 2001–2010 period. Other summers experienced below-average cyclones. No overall trend was found in the counts of cyclones during the study period. Our calculated numbers of cyclones were consistent with the results for the same years from Leibensperger et al. (2008) and Bauer and Del Genio (2006).

In summer, cyclones tend to move around the 500 hPa vortex, which is over the cold Arctic Ocean with broadly symmetric flow around it (Serreze et al., 2007). On the North American side, the high latitude flow on the 500 hPa pressure level has a southward component, which tends to steer systems away from the Arctic Ocean (Fig. 7b). Composite analyses associated with years of strong (2003, 2006, 2008, 2009, and 2010) vs. weak (2001, 2002, 2004, 2005, and 2007) cyclone activities revealed distinct differences in regional to large scale circulation (Fig. 7c). There turned out to be a pronounced positive difference of ∼ 35 gpm centered over Baffin Island (north of the northeast US) and a negative difference of ∼ 25 gpm centered over the northeast

US (Fig. 7c). This difference was related to the negative phase of AO (Fig. 7a), when surface pressure is abnormally high in the polar region and low in the midlatitudes (Archambault et al., 2008). In a negative AO season, Arctic lows and westerlies are weaker, leading to more frequent cold-air outbreaks down to Eurasia and the US, and stormy weather over the Mediterranean (Hess and Lamarque, 2007), and ultimate low baseline CO and O_3 across the northeast US.

A case in point was summer 2009 with the largest cyclone count (20) and the strongest negative AO phase (−0.92) of the decade (Fig. 7a). Consistent with earlier results, the difference of 500 hPa geopotential height between summer 2009 and the 10 year average had negative anomalies up to ∼ −60 gpm over the North American continent and positive anomalies up to ∼ 65 gpm centered near the pole (Fig. 7d). The sea level pressure field (Fig. 7e) featured a pronounced mean low over southern Canada and the streamlines suggested an unusually strong northeasterly component. Indeed, the frequency distribution of wind direction at each site suggested more frequent occurrence of northeasterly wind (22.5–112.5°), with 21 % at PM, 9 % at MWO, 42 % at TF, 11 % at PSP, and 13 % at WFM (Fig. 8). In summer 2009, the northeast US was more often under the influence of cold frontal passages associated with the largest number of cyclones passing through the region. As a result, the northeast US was exposed most frequently to air masses of Arctic origin. Moreover, emissions from large scale wildfires clearly had global effects as discussed in Sect. 3.3.1. In summer 2009, ∼ 11.9 Tg CO, the lowest of the decade, was emitted from wildfires in Russia and Canada (Fig. 7f). Hence, the lowest fire emissions of CO and the most frequent cyclone activities were likely two important factors leading to the lowest summertime baseline CO and O_3 in 2009 at the study sites.

A contrasting case was summer 2003, when AO was negative and 15 cyclones passed the region (Fig. 7a), 25 % greater than the decadal mean (12), and yet baseline CO and O_3 at the sites reached the decadal maxima (Figs. 4c, d and 7f). According to the analysis above, baseline CO and baseline O_3 were expected to be lower during this summer than the decadal average as a result of above-average passages of cyclones.

However, in summer 2003 CO emissions from Russian and Canadian wildfires were the largest of the decade (Sect. 3.3.1), counteracting the effect of the AO. Another interesting example was summer 2007 which had the lowest cyclone activity of the decade (Fig. 7a), and the total CO emissions from wildfires in Russia and Canada were 13.6 Tg, the second lowest of the decade following summer 2009 (Fig. 7f). The site-average baseline CO and O_3 levels in summer 2007 were below the decadal means. Therefore, the effect of biomass burning may dominate over that of AO and cyclone activity during some summers, while the two worked in concert during others.

Overall, no distinct correlation between counts of cyclones and baseline O_3 was found at most sites (AI, CS, MWO, PM, TF, WFM), while no significant correlation between counts of cyclones and baseline CO was found at any of the sites. The only exception was PSP where the count of cyclones was found to be reasonably anti-correlated with baseline O_3 ($r = -0.56$, $p = 0.05$) in the summer. As discussed in Sect. 3.3.1, PSP was the only site that did not seem to be affected by the Russian and Canadian wildfire emissions as all other sites were, possibly due to its being situated in a region less impacted by large-scale dynamics. Perhaps this very dynamic characteristic cast the site under a predominant influence of synoptic systems, e.g., the Bermuda High and cold frontal passages. As commonly known, high mixing ratios of O_3 in the northeast occur under summertime stagnant, clear sky conditions associated with the Bermuda High (Logan, 1989; Vukovich, 1995; Hegarty et al., 2007; Lai et al., 2012), while low O_3 was often linked to cold fronts which sweep out polluted air leaving much cooler and cleaner air in the northeast (Cooper et al., 2001; Leibensperger et al., 2008; Li et al., 2005). Conceivably, with more frequent cyclones passing the northeast US, lower concentrations of baseline CO and O_3 would be expected, and the predominant effect of such synoptic systems could quite likely lead to anticorrelation between the baseline CO/O_3 levels and cyclone activities.

3.3.3 Impact of NAO in spring (March and April)

Wildfires in March and April were scarce, with mean CO emissions of 1.78 Tg in Russia and 0.004 Tg in Canada over 2001–2010, negligible compared to emissions during the fire season (May–September). To focus on the impact of large circulation patterns on baseline CO and O_3 in spring, the May data were excluded to avoid the effect of biomass burning. Springtime baseline O_3 at each site showed strong and consistent interannual variation up to 10 ppbv (Fig. 9a). The baseline O_3 mixing ratio averaged at all the seven sites over the decade was 46.5 ppbv, and exceeded the average (> 46.5 ppbv) in 2001, 2003, 2005, 2008, 2010, and was below average (≤ 46.5 ppbv) in 2002, 2004, 2006, 2007, 2009 (Fig. 9a).

The difference of 850 hPa geopotential height between the lower and higher O_3 years is shown in Fig. 10. There was a pronounced difference up to 40 gpm in the Bermuda/Azores high and ∼ −40 gpm in the Icelandic low, which resulted in stronger gradient flow between the two pressure systems, known as the positive phase of NAO. Over 2001–2010, NAO index was significantly positive in 2002, 2004, 2007, 2009 and negative in 2001, 2005, 2008, 2010, which corresponded mostly to the years of below and above the decadal average baseline O_3, respectively. Significant negative correlation was found between the NAO index and baseline O_3 at each site (CS: $r = -0.75$, $p = 0.03$; MWO: $r = -0.68$, $p = 0.03$; PM: $r = -0.81$, $p = 0.03$; TF: $r = -0.81$, $p < 0.01$; PSP: $r = -0.58$, $p = 0.06$; WFM: $r = -0.51$, $p = 0.10$). The negative correlation between baseline O_3 and the NAO index could be a result of multiple factors, such as solar flux, stratosphere-tropospheric exchange, and continental export of O_3 produced in North America. It should be noted that, no significant correlation was found between the NAO index and baseline CO at any of the sites, which suggests that NAO is not linked to or played an insignificant role in the interannual variability of baseline CO.

The first possible explanation for the baseline O_3 and NAO index anticorrelation was changes in surface solar radiation flux during positive/negative NAO years. During a positive NAO year, the mean North Atlantic storm track parallels the eastern

North American coastline before extending northeastward to near Iceland (Rogers, 1997). This storm track and its associated moisture transport and convergence lead to relatively wet conditions near the eastern US coast (Archambault et al., 2008; Hurrell, 1995). During a negative NAO year, the mean North Atlantic storm track is more zonal (Rogers, 1997), leading to relatively dry conditions near the eastern US coast (Archambault et al., 2008; Hurrell, 1995). At our costal sites, significant correlation was found between relative humidity and the NAO index (CS: $r = 0.85$, $p = 0.02$; TF: $r = 0.64$,$p = 0.06$), while the correlation was weaker at inland, elevated sites (PSP: $r = 0.23$, $p = 0.26$; WFM: $r = 0.40$, $p = 0.13$) (Fig. 9b).

During positive NAO years, wetter conditions indicate higher relative humidity and more cloudiness, most likely leading to reduced solar radiation flux near the surface and subsequently less O_3 production. As expected, a significant negative correlation was found between relative humidity and solar radiation ($r = -0.67$, $p = 0.05$) (Fig. 9b) and a significant positive correlation between baseline O_3 and solar radiation flux ($r = 0.75$, $p = 0.03$) at TF in March and April. No significant correlation between these variables was found in other seasons.

Another possible explanation for the negative correlation between NAO index and baseline O_3 was the influence of stratospheric intrusion. Dynamically, the North American trough induces descending air on its tailing side and in the upper troposphere it can cause tropopause folding with stratospheric air mixing downward into the troposphere. The difference of the PV patterns between positive NAO years and negative NAO years is illustrated in Fig. 11. Negative anomalies of $\sim -0.6\times 10^{-9}\,m^2\,s^{-1}$ kg were found over the northeast US, suggesting that positive NAO was related to less stratospheric intrusion (Hess and Lamarque, 2007) over the northeast US. This is consistent with lower baseline O_3 levels during positive NAO springs. This was further verified using the stratospheric O_3 dataset constructed by Liu et al. (2013). Stratospheric O_3 was hardly detected at the lowest two layers (i.e., 0.5 and 1.5 km) in April. In March, $\sim$ 40–60 ppbv of stratospheric O_3 reached the lowest layer in our study area in 2004 and 2006–2008 and reached the 1.5 km layer in 2001–2008. The stratospheric contribution to the 0.5 km layer was the largest in March 2008, when NAO was negative (Fig. 9).

The third possible factor affecting baseline O_3 over the northeast US was the effect of North American continental export. During a positive NAO phase, the anticyclonic circulation off the US east coast and the cyclonic circulation across the North Atlantic were amplified with a northward shift (Rogers, 1997). As a result, stronger surface wind was found near 50° N across the North Atlantic basin and into Northern Europe (Hess and Lamarque, 2007). Annual wind speed from the west (247.5–337.5°) was calculated at the study sites (Fig. 9c). Positive correlation was found between surface wind and NAO index at most sites (MWO: $r = 0.76$, $p = 0.02$; CS: $r = 0.68$, $p = 0.06$; TF: $r = 0.57$, $p = 0.09$). Eckhardt et al. (2004) found that the warm conveyor belt over the northeast US coast occurred $\sim$ 12 % more frequently in positive NAO years than in negative NAO years. The ending trajectories of the warm conveyor belt in positive NAO years extended further eastward into western and northern Europe (Eckhardt et al., 2004). It was suggested that in a positive NAO year, the O_3 produced over the northeast US was less likely accumulated in the region, and was more likely transported faster off the continent and across the Atlantic Ocean. These changes were consistent with the positive anomalies of O_3 observed over northwestern Europe (Christoudias et al., 2012; Eckhardt et al., 2003).

4 Summary

Baseline CO and O_3 at seven rural sites in the northeast US were examined for their seasonal and interannual variabilities during the time period of 2001–2010, and potential mechanisms controlling the variabilities were investigated. It was found that baseline CO at most sites (MWO, PM, TF, PSP, and WFM) decreased significantly at a rate between -4.3 to -2.3 ppbv yr^{-1}, while baseline O_3 was relatively constant. No trends were found in baseline O_3 at all sites probably resulting from relatively constant mixing

ratios of CH_4 in the 2000s and opposite rates of change in NO_x emissions around the world.

In spring and winter, baseline CO at MWO and WFM did not exhibit a significant trend, possibly a result of the combined effect of decreasing emissions in the northeast US and increasing emissions in Asia. TF, a coastal rural site, was the only location where baseline O_3 was found to increase significantly at a rate of 2.4 and 2.7 ppbv yr^{-1} in spring and winter, respectively, most likely caused by the decrease in NO_x emissions over the urban corridor.

It was found that interannual variations of baseline CO and O_3 were predominantly influenced by biomass burning emissions, cyclone activities, and NAO. In summer, ~ 38 % of baseline CO variability was attributed to CO emissions from forest fires in Russia and ~ 22 % to emissions from forest fires in Canada. The lowest mixing ratios of baseline CO and O_3 at most sites in summer 2009 were linked to frequent cyclone activity, which were induced by the unusually weak low pressure system in the Arctic region. In spring, a significant negative correlation was found between baseline O_3 and the NAO index, potentially due to variations of solar flux, stratospheric intrusion, and continental export.

In December 2014, the U.S. EPA proposed to tighten the 2008 NAAQS for daily maximum 8 h average O_3 from 75 ppbv to a level within a range of 65–70 ppbv to provide protection of public health and welfare (EPA, 2014). As the O_3 NAAQS are set closer to background levels, states will face ever increasing challenges with regard to fulfilling their obligation for NAAQS attainment. Through this study it was reinforced that, in addition to domestic emission control, intercontinental transport of anthropogenic emissions and wildfires emissions together with meteorological conditions should be considered for an encompassing, cost-effective emission control strategy that accounts for impacts of regional to global emissions and moreover emissions of multi-pollutants (e.g. CO, CH_4 NO_x, and NMHCs). In addition, the relationships between baseline O_3/CO and various factors (e.g. NO_x emission controls, biomass burning emissions, NAO, and AO) examined in this study can also be used as reference point for evaluating

global/regional air quality modeling systems that are used in air quality management applications. One limitation of this study is that it was based on ten-year observations, and hence it was unlikely to predict the potential changes in natural emissions and AO/NAO signals as well as their impacts on baseline O_3. Future research is warranted to further address the issues identified in this work on climatological time scales.

Acknowledgements. This work was funded by the Environment Protection Agency grant #83521501. We are grateful to Z. Ye, Y. Zhang, R. D. Yanai, G. Townsend, and E. P. Law for their valuable suggestions and help. We thank K. Cochrane and K. Yan for their assistance in the early stage of the study.

Disclaimer. Although this work has been reviewed and approved for publication by the U.S. Environmental Protection Agency (EPA), it does not reflect the views and policies of the agency.

References

Archambault, H. M., Bosart, L. F., Keyser, D., and Aiyyer, A. R.: Influence of large-scale flow regimes on cool-season precipitation in the northeastern United States, Mon. Weather Rev., 136, 2945–2963, doi:10.1175/2007MWR2308.1, 2008.

Bae, M. S., Schwab, J. J., Chen, W. N., Lin, C. Y., Rattigan, O. V., and Demerjian, K. L.: Identifying pollutant source directions using multiple analysis methods at a rural location in New York, Atmos. Environ., 45, 2531–2540, doi:10.1016/j.atmosenv.2011.02.020, 2011.

Barnston, A. G. and Livezey, R. E.: Classification, seasonality and persistence of low-frequency atmospheric circulation patterns, Mon. Weather Rev., 115, 1083–1126, 1987.

Bauer, M. and Del Genio, A. D.: Composite analysis of winter cyclones in a GCM: influence on climatological humidity, J. Climate, 19, 1652–1672, doi:10.1175/JCLI3690.1, 2006.

Bell, M. L., Goldberg, R., Hogrefe, C., Kinney, P. L., Knowlton, K., Lynn, B., Rosenthal, J., Rosenzweig, C., and Patz, J. A.: Climate change, ambient ozone, and health in 50 US cities, Clim. Change, 82, 61–76, doi:10.1007/s10584-006-9166-7, 2007.

Brand, S., Dethloff, K., and Handorf, D.: Tropospheric circulation sensitivity to an interactive stratospheric ozone, Geophys. Res. Lett., 35, 1–5, doi:10.1029/2007GL032312, 2008.

Brandt, R. E., Schwab, J. J., Casson, P. W., Roychowdhury, U. K., Wolfe, D., Demerjian, K. L., Civerolo, K. L., Rattigan, O. V., and Felton, H. D.: Atmospheric chemistry measurements at Whiteface Mountain, NY: ozone and reactive trace gases, Aerosol and Air Quality Research, submitted to special issue, 2015.

Buckley, S. M. and Mitchell, M. J.: Improvements in urban air quality: case studies from New York state, USA, Water Air Soil Poll., 214, 93–106, doi:10.1007/s11270-010-0407-z, 2011.

Chan, E.: Regional ground-level ozone trends in the context of meteorological influences across Canada and the eastern United States from 1997 to 2006, J. Geophys. Res.-Atmos., 114, 1–18, doi:10.1029/2008JD010090, 2009.

Chan, E. and Vet, R. J.: Baseline levels and trends of ground level ozone in Canada and the United States, Atmos. Chem. Phys., 10, 8629–8647, doi:10.5194/acp-10-8629-2010, 2010.

Christoudias, T., Pozzer, A., and Lelieveld, J.: Influence of the North Atlantic Oscillation on air pollution transport, Atmos. Chem. Phys., 12, 869–877, doi:10.5194/acp-12-869-2012, 2012.

Cooper, O. R., Moody, J. L., Parrish, D. D., Trainer, M., Ryerson, T. B., Holloway, J. S., Hübler, G., Fehsenfeld, F. C., Oltmans, S. J., and Evans, M. J.: Trace gas signatures of the airstreams within North Atlantic cyclones: case studies from the North Atlantic Regional Experiment (NARE '97) aircraft intensive, J. Geophys. Res.-Atmos., 106, 5437–5456, doi:10.1029/2000JD900574, 2001.

Cooper, O. R., Parrish, D. D., Stohl, A., Trainer, M., Nédélec, P., Thouret, V., Cammas, J. P., Oltmans, S. J., Johnson, B. J., Tarasick, D., Leblanc, T., McDermid, I. S., Jaffe, D., Gao, R., Stith, J., Ryerson, T., Aikin, K., Campos, T., Weinheimer, A., and Avery, M. A.: Increasing springtime ozone mixing ratios in the free troposphere over western North America, Nature, 463, 344–348, doi:10.1038/nature08708, 2010.

Cooper, O. R., Gao, R. S., Tarasick, D., Leblanc, T., and Sweeney, C.: Long-term ozone trends at rural ozone monitoring sites across the United States, 1990–2010, J. Geophys. Res.-Atmos., 117, 1990–2010, doi:10.1029/2012JD018261, 2012.

Creilson, J. K., Fishman, J., and Wozniak, A. E.: Intercontinental transport of tropospheric ozone: a study of its seasonal variability across the North Atlantic utilizing tropospheric ozone residuals and its relationship to the North Atlantic Oscillation, Atmos. Chem. Phys., 3, 2053–2066, doi:10.5194/acp-3-2053-2003, 2003.

Creilson, J. K., Fishman, J., and Wozniak, A. E.: Arctic oscillation-induced variability in satellite-derived tropospheric ozone, Geophys. Res. Lett., 32, 1–5, doi:10.1029/2005GL023016, 2005.

Cui, J., Pandey Deolal, S., Sprenger, M., Henne, S., Staehelin, J., Steinbacher, M., and Nédélec, P.: Free tropospheric ozone changes over Europe as observed at Jungfraujoch (1990–2008): an analysis based on backward trajectories, J. Geophys. Res.-Atmos., 116, 1–14, doi:10.1029/2010JD015154, 2011.

Daniel, J. S. and Solomon, S.: On the climate forcing of carbon monoxide, J. Geophys. Res.-Atmos., 103, 13249–13260, doi:10.1029/98JD00822, 1998.

Derwent, R. G., Simmonds, P. G., Manning, A. J., and Spain, T. G.: Trends over a 20-year period from 1987 to 2007 in surface ozone at the atmospheric research station, Mace Head, Ireland, Atmos. Environ., 41, 9091–9098, doi:10.1016/j.atmosenv.2007.08.008, 2007.

Duncan, B. N. and Bey, I.: A modeling study of the export pathways of pollution from Europe: seasonal and interannual variations (1987–1997), J. Geophys. Res.-Atmos., 109, D08301, doi:10.1029/2003JD004079, 2004.

Dutkiewicz, V. A., Husain, L., Roychowdhury, U. K., and Demerjian, K. L.: Impact of Canadian wildfire smoke on air quality at two rural sites in NY state, Atmos. Environ., 45, 2028–2033, doi:10.1016/j.atmosenv.2011.01.072, 2011.

Eckhardt, S., Stohl, A., Beirle, S., Spichtinger, N., James, P., Forster, C., Junker, C., Wagner, T., Platt, U., and Jennings, S. G.: The North Atlantic Oscillation controls air pollution transport to the Arctic, Atmos. Chem. Phys., 3, 1769–1778, doi:10.5194/acp-3-1769-2003, 2003.

Eckhardt, S., Stohl, A., Wernli, H., James, P., Forster, C., and Spichtinger, N.: A 15-year climatology of warm conveyor belts, J. Climate, 17, 218–237, 2004.

Emmons, L. K., Hess, P., Klonecki, A., Tie, X., Horowitz, L., Lamarque, J.-F., Kinnison, D., Brasseur, G., Atlas, E., Browell, E., Cantrell, C., Eisele, F., Mauldin, R. L., Merrill, J., Ridley, B., and Shetter, R.: Budget of tropospheric ozone during TOPSE from two chemical transport models, J. Geophys. Res.-Atmos., 108, 8372, doi:10.1029/2002JD002665, 2003.

Fiore, A. M., Jacob, D. J., Bey, I., Yantosca, R. M., Field, B. D., Fusco, A. C., and Wilkinson, J. G.: Background ozone over the United States in summer: origin, trend, and contribution to pollution episodes, J. Geophys. Res.-Atmos., 107, ACH 11-1–ACH 11-25, doi:10.1029/2001JD000982, 2002.

Frost, G. J., McKeen, S. A., Trainer, M., Ryerson, T. B., Neuman, J. A., Roberts, J. M., Swanson, A., Holloway, J. S., Sueper, D. T., Fortin, T., Parrish, D. D., Fehsenfeld, F. C., Flocke, F., Peckham, S. E., Grell, G. A., Kowal, D., Cartwright, J., Auerbach, N., and Habermann, T.: Effects of changing power plant NO_x emissions on ozone in the eastern United States: proof of concept, J. Geophys. Res.-Atmos., 111, D12306, doi:10.1029/2005JD006354, 2006.

Granier, C., Bessagnet, B., Bond, T., D'Angiola, A., van der Gon, H. D., Frost, G. J., Heil, A., Kaiser, J. W., Kinne, S., Klimont, Z., Kloster, S., Lamarque, J. F., Liousse, C., Masui, T., Meleux, F., Mieville, A., Ohara, T., Raut, J. C., Riahi, K., Schultz, M. G., Smith, S. J., Thompson, A., van Aardenne, J., van der Werf, G. R., and van Vuuren, D. P.: Evolution of anthropogenic and biomass burning emissions of air pollutants at global and regional scales during the 1980–2010 period, Clim. Change, 109, 163–190, doi:10.1007/s10584-011-0154-1, 2011.

Gratz, L. E., Jaffe, D. A., and Hee, J. R.: Causes of increasing ozone and decreasing carbon monoxide in springtime at the Mt. Bachelor Observatory from 2004 to 2013, Atmos. Environ., 109, 323–330, doi:10.1016/j.atmosenv.2014.05.076, 2014.

Harden, J. W., Trumbore, S. E., Stocks, B. J., Hirsch, A., Gower, S. T., O'Neill, K. P., and Kasischke, E. S.: The role of fire in the boreal carbon budget, Glob. Change Biol., 6 (Supplement 1), 174–184, doi:10.1046/j.1365-2486.2000.06019.x, 2000.

Hecobian, A., Liu, Z., Hennigan, C. J., Huey, L. G., Jimenez, J. L., Cubison, M. J., Vay, S., Diskin, G. S., Sachse, G. W., Wisthaler, A., Mikoviny, T., Weinheimer, A. J., Liao, J., Knapp, D. J., Wennberg, P. O., Kürten, A., Crounse, J. D., Clair, J. St., Wang, Y., and Weber, R. J.: Comparison of chemical characteristics of 495 biomass burning plumes intercepted by the NASA DC-8 aircraft during the ARCTAS/CARB-2008 field campaign, Atmos. Chem. Phys., 11, 13325–13337, doi:10.5194/acp-11-13325-2011, 2011.

Hegarty, J., Mao, H., and Talbot, R.: Synoptic controls on summertime surface ozone in the northeastern United States, J. Geophys. Res.-Atmos., 112, D14306, doi:10.1029/2006JD008170, 2007.

Hegarty, J., Mao, H., and Talbot, R.: Synoptic influences on springtime tropospheric O_3 and CO over the North American export region observed by TES, Atmos. Chem. Phys., 9, 3755–3776, doi:10.5194/acp-9-3755-2009, 2009.

Herron-Thorpe, F. L., Mount, G. H., Emmons, L. K., Lamb, B. K., Jaffe, D. A., Wigder, N. L., Chung, S. H., Zhang, R., Woelfle, M. D., and Vaughan, J. K.: Air quality simulations of wildfires in the Pacific Northwest evaluated with surface and satellite observations during the summers of 2007 and 2008, Atmos. Chem. Phys., 14, 12533–12551, doi:10.5194/acp-14-12533-2014, 2014.

Hess, P. G. and Lamarque, J. F.: Ozone source attribution and its modulation by the Arctic oscillation during the spring months, J. Geophys. Res.-Atmos., 112, 1–17, doi:10.1029/2006JD007557, 2007.

Honrath, R. E., Owen, R. C., Val Martín, M., Reid, J. S., Lapina, K., Fialho, P., Dziobak, M. P., Kleissl, J., and Westphal, D. L.: Regional and hemispheric impacts of anthropogenic and biomass burning emissions on summertime CO and O_3 in the North Atlantic lower free troposphere, J. Geophys. Res.-Atmos., 109, 1–17, doi:10.1029/2004JD005147, 2004.

Task Force on Hemispheric Transport of Air Pollution (TF HTAP): Hemispheric transport of air pollution 2010 assessment report, edited by: Keating, T. J. and Zuber, A., draft, available at: http://www.htap.org, 2010.

Hu, Q., Tawaye, Y., and Feng, S.: Variations of the Northern Hemisphere atmospheric energetics: 1948–2000, J. Climate, 17, 1975–1986, doi:10.1175/1520-0442(2004)017<1975:VOTNHA>2.0.CO;2, 2004.

Hurrell, J. W.: Decadal trends in the north atlantic oscillation: regional temperatures and precipitation, Science, 269, 676–679, doi:10.1126/science.269.5224.676, 1995.

Intergovernmental Panel on Climate Change (IPCC): Climate Change 2001: The Scientific Basis, Clim. Change 2001 Sci. Basis, 881, doi:10.1256/004316502320517344, 2001.

Intergovernmental Panel on Climate Change (IPCC), Climate Change 2007: The Physical Science Basis, in: Contribution of Working Group I to the Fourth Assessment Report of the Intergovernmental Panel on Climate Change, edited by: Solomon, S., Qin, D., Manning, M., Chen, Z., Marquis, M., Averyt, K. B., Tignor M., and Miller H. L., Cambridge University Press, Cambridge, UK and New York, NY, USA, 2007.

Jacob, D. J.: Seasonal transition from NO_x- to hydrocarbon-limited conditions for ozone production over the eastern United States in september, J. Geophys. Res., 100, 9315–9324, doi:10.1029/94JD03125, 1995.

Jaffe, D., Bertschi, I., Jaeglé, L., Novelli, P., Reid, J. S., Tanimoto, H., Vingarzan, R., and Westphal, D. L.: Long-range transport of Siberian biomass burning emissions and impact on surface ozone in western North America, Geophys. Res. Lett., 31, 6–9, doi:10.1029/2004GL020093, 2004.

James, P., Stohl, A., Forster, C., Eckhardt, S., Seibert, P., and Frank, A.: A 15-year climatology of stratosphere–troposphere exchange with a Lagrangian particle dispersion model 2. Mean climate and seasonal variability, J. Geophys. Res.-Atmos., 108, 8522, doi:10.1029/2002JD002639, 2003.

Jonson, J. E., Simpson, D., Fagerli, H., and Solberg, S.: Can we explain the trends in European ozone levels?, Atmos. Chem. Phys., 6, 51–66, doi:10.5194/acp-6-51-2006, 2006.

Kang, C. M., Gold, D., and Koutrakis, P.: Downwind O_3 and $PM_{2.5}$ speciation during the wildfires in 2002 and 2010, Atmos. Environ., 95, 511–519, doi:10.1016/j.atmosenv.2014.07.008, 2014.

Kim, S.-W., Heckel, A., McKeen, S. A., Frost, G. J., Hsie, E.-Y., Trainer, M. K., Richter, A., Burrows, J. P., Peckham, S. E., and Grell, G. A.: Emission reductions and their impact on air quality, Geophys. Res. Lett., 33, 1–5, doi:10.1029/2006GL027749, 2006.

Kondragunta, S., Lee, P., McQueen, J., Kittaka, C., Prados, A. I., Ciren, P., Laszlo, I., Pierce, R. B., Hoff, R., and Szykman, J. J.: Air quality forecast verification using satellite data, J. Appl. Meteorol. Clim., 47, 425–442, doi:10.1175/2007JAMC1392.1, 2008.

Kopacz, M., Jacob, D. J., Fisher, J. A., Logan, J. A., Zhang, L., Megretskaia, I. A., Yantosca, R. M., Singh, K., Henze, D. K., Burrows, J. P., Buchwitz, M., Khlystova, I., McMillan, W. W., Gille, J. C., Edwards, D. P., Eldering, A., Thouret, V., and Nedelec, P.: Global estimates of CO sources with high resolution by adjoint inversion of multiple satellite datasets (MOPITT, AIRS, SCIAMACHY, TES), Atmos. Chem. Phys., 10, 855–876, doi:10.5194/acp-10-855-2010, 2010.

Krichak, S. O. and Alpert, P.: Signatures of the NAO in the atmospheric circulation during wet winter months over the Mediterranean region, Theor. Appl. Climatol., 82, 27–39, doi:10.1007/s00704-004-0119-7, 2005.

Kumar, A., Wu, S., Weise, M. F., Honrath, R., Owen, R. C., Helmig, D., Kramer, L., Val Martin, M., and Li, Q.: Free-troposphere ozone and carbon monoxide over the North Atlantic for 2001–2011, Atmos. Chem. Phys., 13, 12537–12547, doi:10.5194/acp-13-12537-2013, 2013.

Lai, T. L., Talbot, R., and Mao, H.: An investigation of two highest ozone episodes during the last decade in New England, Atmosphere, 3, 59–86, doi:10.3390/atmos3010059, 2012.

Lamarque, J.-F., and Hess, P. G.: Arctic Oscillation modulation of the Northern Hemisphere spring tropospheric ozone, Geophys. Res. Lett., 31, L06127, doi:10.1029/2003GL019116, 2004.

Lefohn, A. S., Shadwick, D., and Oltmans, S. J.: Characterizing changes in surface ozone levels in metropolitan and rural areas in the United States for 1980–2008 and 1994–2008, Atmos. Environ., 44, 5199–5210, doi:10.1016/j.atmosenv.2010.08.049, 2010.

Leibensperger, E. M., Mickley, L. J., and Jacob, D. J.: Sensitivity of US air quality to mid-latitude cyclone frequency and implications of 1980–2006 climate change, Atmos. Chem. Phys., 8, 7075–7086, doi:10.5194/acp-8-7075-2008, 2008.

Liang, Q., Jaeglé, L., Jaffe, D. A., Weiss-Penzias, P., Heckman, A., and Snow, J. A.: Long-range transport of Asian pollution to the northeast Pacific: seasonal variations and transport pathways of carbon monoxide, J. Geophys. Res.-Atmos., 109, 1–16, doi:10.1029/2003JD004402, 2004.

Li, Q., Jacob, D. J., Bey, I., Palmer, P. I., Duncan, B. N., Field, B. D., Martin, R. V., Fiore, A. M., Yantosca, R. M., Parrish, D. D., Simmonds, P. G. and Oltmans, S. J.: Transatlantic transport of pollution and its effects on surface ozone in Europe and North America, J. Geophys. Res.-Atmos., 107, ACH 4-1–ACH 4-21, doi:10.1029/2001JD001422, 2002.

Li, Q., Jacob, D. J., Park, R., Wang, Y., Heald, C. L., Hudman, R., Yantosca, R. M., Martin, R. V., and Evans, M.: North American pollution outflow and the trapping of convectively lifted pollution by upper-level anticyclone, J. Geophys. Res.-Atmos., 110, D10301, doi:10.1029/2004JD005039, 2005.

Lin, C.-Y. C., Jacob, D. J., Munger, J. W., and Fiore, A. M.: Increasing background ozone in surface air over the United States, Geophys. Res. Lett., 27, 3465–3468, doi:10.1029/2000GL011762, 2000.

Liu, J., Tarasick, D. W., Fioletov, V. E., McLinden, C., Zhao, T., Gong, S., Sioris, C., Jin, J. J., Liu, G., and Moeini, O.: A global ozone climatology from ozone soundings via trajectory mapping: a stratospheric perspective, Atmos. Chem. Phys., 13, 11441–11464, doi:10.5194/acp-13-11441-2013, 2013.

Liu, S. C.: Ozone production in the rural troposphere and the implications for regional and global ozone distributions., J. Geophys. Res., 92, 4191–4207, 1987.

Logan, J. A.: Ozone in rural areas of the United States, J. Geophys. Res., 94, 8511–8532, 1989.

Logan, J. A., Staehelin, J., Megretskaia, I. A., Cammas, J. P., Thouret, V., Claude, H., De Backer, H., Steinbacher, M., Scheel, H. E., Stbi, R., Fröhlich, M., and Derwent, R.: Changes in ozone over Europe: analysis of ozone measurements from sondes, regular aircraft (MOZAIC) and alpine surface sites, J. Geophys. Res.-Atmos., 117, 1–23, doi:10.1029/2011JD016952, 2012.

Mao, H. and Talbot, R.: Role of meteorological processes in two New England ozone episodes during summer 2001, J. Geophys. Res.-Atmos., 109, 1–17, doi:10.1029/2004JD004850, 2004.

Mao, H. and Talbot, R.: Speciated mercury at marine, coastal, and inland sites in New England – Part 1: Temporal variability, Atmos. Chem. Phys., 12, 5099–5112, doi:10.5194/acp-12-5099-2012, 2012.

Mathur, R.: Estimating the impact of the 2004 Alaskan forest fires on episodic particular matter polllution over the eastern United States through assimilation of satellite-derived aerosol optical depths in a regional air quality model, J. Geophys. Res.-Atmos., 113, D17302, doi:10.1029/2007JD009767, 2008.

McKendry, I., Strawbridge, K., Karumudi, M. L., O'Neill, N., Macdonald, A. M., Leaitch, R., Jaffe, D., Cottle, P., Sharma, S., Sheridan, P., and Ogren, J.: Californian forest fire plumes over Southwestern British Columbia: lidar, sunphotometry, and mountaintop chemistry observations, Atmos. Chem. Phys., 11, 465–477, doi:10.5194/acp-11-465-2011, 2011.

Miller, S. M., Matross, D. M., Andrews, A. E., Millet, D. B., Longo, M., Gottlieb, E. W., Hirsch, A. I., Gerbig, C., Lin, J. C., Daube, B. C., Hudman, R. C., Dias, P. L. S., Chow, V. Y., and Wofsy, S. C.: Sources of carbon monoxide and formaldehyde in North America determined from high-resolution atmospheric data, Atmos. Chem. Phys., 8, 7673–7696, doi:10.5194/acp-8-7673-2008, 2008.

Monks, P.: A review of the observations and origins of the spring ozone maximum, Atmos. Environ., 34, 3545–3561, doi:10.1016/S1352-2310(00)00129-1, 2000.

Murazaki, K. and Hess, P.: How does climate change contribute to surface ozone change over the United States?, J. Geophys. Res.-Atmos., 111, 1–16, doi:10.1029/2005JD005873, 2006.

Novelli, P. C., Masarie, K. A., Lang, P. M., Hall, B. D., Myers, R. C., and Elkins, J. W.: Reanalysis of tropospheric CO trends: effects of the 1997–1998 wildfires, J. Geophys. Res.-Atmos., 108, ACH 14-1–ACH 14-14, 2003.

Oltmans, S. J., Lefohn, A. S., Harris, J. M., and Shadwick, D. S.: Background ozone levels of air entering the west coast of the US and assessment of longer-term changes, Atmos. Environ., 42, 6020–6038, doi:10.1016/j.atmosenv.2008.03.034, 2008.

Oltmans, S. J., Lefohn, A. S., Harris, J. M., Tarasick, D. W., Thompson, A. M., Wernli, H., Johnson, B. J., Novelli, P. C., Montzka, S. A., Ray, J. D., Patrick, L. C., Sweeney, C., Jefferson, A., Dann, T., Davies, J., Shapiro, M., and Holben, B. N.: Enhanced ozone over western North America from biomass burning in Eurasia during April 2008 as seen in surface and profile observations, Atmos. Environ., 44, 4497–4509, doi:10.1016/j.atmosenv.2010.07.004, 2010.

Oltmans, S. J., Lefohn, A. S., Shadwick, D., Harris, J. M., Scheel, H. E., Galbally, I., Tarasick, D. W., Johnson, B. J., Brunke, E. G., Claude, H., Zeng, G., Nichol, S., Schmidlin, F.,

Davies, J., Cuevas, E., Redondas, A., Naoe, H., Nakano, T., and Kawasato, T.: Recent tropospheric ozone changes – a pattern dominated by slow or no growth, Atmos. Environ., 67, 331–351, doi:10.1016/j.atmosenv.2012.10.057, 2013.

Oswald, E. M., Dupigny-Giroux, L.-A., Leibensperger, E. M., Poirot, R., and Merrell, J.: Climate controls on air quality in the northeastern U.S.: an examination of summertime ozone statistics during 1993–2012, Atmos. Environ., 112, 278–288, doi:10.1016/j.atmosenv.2015.04.019, 2015.

Parrish, D. D., Singh, H. B., Molina, L., and Madronich, S.: Air quality progress in North American megacities: a review, Atmos. Environ., 45, 7015–7025, doi:10.1016/j.atmosenv.2011.09.039, 2011.

Parrish, D. D., Law, K. S., Staehelin, J., Derwent, R., Cooper, O. R., Tanimoto, H., Volz-Thomas, A., Gilge, S., Scheel, H.-E., Steinbacher, M., and Chan, E.: Long-term changes in lower tropospheric baseline ozone concentrations at northern mid-latitudes, Atmos. Chem. Phys., 12, 11485–11504, doi:10.5194/acp-12-11485-2012, 2012.

Parrish, D. D., Law, K. S., Staehelin, J., Derwent, R., Cooper, O. R., Tanimoto, H., Volz-Thomas, A., Gilge, S., Scheel, H. E., Steinbacher, M., and Chan, E.: Lower tropospheric ozone at northern midlatitudes: changing seasonal cycle, Geophys. Res. Lett., 40, 1631–1636, doi:10.1002/grl.50303, 2013.

Pausata, F. S. R., Pozzoli, L., Vignati, E., and Dentener, F. J.: North Atlantic Oscillation and tropospheric ozone variability in Europe: model analysis and measurements intercomparison, Atmos. Chem. Phys., 12, 6357–6376, doi:10.5194/acp-12-6357-2012, 2012.

Penkett, S. A., Blake, N. J., Lightman, P., Marsh, A. R. W., Anwyl, P., and Butcher, G.: The seasonal variation of nonmethane hydrocarbons in the free troposphere over the North Atlantic Ocean: possible evidence for extensive reaction of hydrocarbons with the nitrate radical, J. Geophys. Res., 98, 2865–2885, 1993.

Petrenko, V. V., Martinerie, P., Novelli, P., Etheridge, D. M., Levin, I., Wang, Z., Blunier, T., Chappellaz, J., Kaiser, J., Lang, P., Steele, L. P., Hammer, S., Mak, J., Langenfelds, R. L., Schwander, J., Severinghaus, J. P., Witrant, E., Petron, G., Battle, M. O., Forster, G., Sturges, W. T., Lamarque, J.-F., Steffen, K., and White, J. W. C.: A 60 yr record of atmospheric carbon monoxide reconstructed from Greenland firn air, Atmos. Chem. Phys., 13, 7567–7585, doi:10.5194/acp-13-7567-2013, 2013.

Pfister, G., Hess, P. G., Emmons, L. K., Lamarque, J.-F., Wiedinmyer, C., Edwards, D. P., Pétron, G., Gille, J. C., and Sachse, G. W.: Quantifying CO emissions from the 2004 Alaskan

wildfires using MOPITT CO data, Geophys. Res. Lett., 32, 1–5, doi:10.1029/2005GL022995, 2005.
Pollack, I. B., Ryerson, T. B., Trainer, M., Neuman, J. A., Roberts, J. M., and Parrish, D. D.: Trends in ozone, its precursors, and related secondary oxidation products in Los Angeles, California: a synthesis of measurements from 1960 to 2010, J. Geophys. Res.-Atmos., 118, 5893–5911, doi:10.1002/jgrd.50472, 2013.
Price, H. U., Jaffe, D. A., Cooper, O. R., and Doskey, P. V.: Photochemistry, ozone production, and dilution during long-range transport episodes from Eurasia to the northwest United States, J. Geophys. Res.-Atmos., 109, 1–10, doi:10.1029/2003JD004400, 2004.
Prinn, R. G.: The Cleansing Capacity of the Atmosphere, Annu. Rev. Environ. Resour., 28, 29–57, doi:10.1146/annurev.energy.28.011503.163425, 2003.
Racherla, P. N. and Adams, P. J.: The response of surface ozone to climate change over the Eastern United States, Atmos. Chem. Phys., 8, 871–885, doi:10.5194/acp-8-871-2008, 2008.
Real, E., Law, K. S., Weinzierl, B., Fiebig, M., Petzold, A., Wild, O., Methven, J., Arnold, S. A., Stohl, A., Huntrieser, H., Roiger, A. E., Schlager, H., Stewart, D., Avery, M. A., Sachse, G. W., Browell, E. V., Ferrare, R. A., and Blake, D.: Processes influencing ozone levels in Alaskan forest fire plumes during long-range transport over the North Atlantic, J. Geophys. Res.-Atmos., 112, 1–19, doi:10.1029/2006JD007576, 2007.
Reidmiller, D. R., Jaffe, D. A., Chand, D., Strode, S., Swartzendruber, P., Wolfe, G. M., and Thornton, J. A.: Interannual variability of long-range transport as seen at the Mt. Bachelor observatory, Atmos. Chem. Phys., 9, 557–572, doi:10.5194/acp-9-557-2009, 2009.
Rogers, J. C.: North Atlantic storm track variability and its association to the North Atlantic oscillation and climate variability of northern Europe, J. Climate, 10, 1635–1647, doi:10.1175/1520-0442(1997)010<1635:NASTVA>2.0.CO;2, 1997.
Schwab, J. J., Spicer, J. B., and Demerjian, K. L.: Ozone, trace gas, and particulate matter measurements at a rural site in southwestern New York state: 1995–2005, J. Air Waste Manage., 59, 293–309, doi:10.3155/1047-3289.59.3.293, 2009.
Serreze, M. C., Barrett, A. P., Slater, A. G., Steele, M., Zhang, J., and Trenberth, K. E.: The large-scale energy budget of the Arctic, J. Geophys. Res.-Atmos., 112, 1–17, doi:10.1029/2006JD008230, 2007.
Stevenson, D. S., Dentener, F. J., Schultz, M. G., Ellingsen, K., van Noije, T. P. C., Wild, O., Zeng, G., Amann, M., Atherton, C. S., Bell, N., Bergmann, D. J., Bey, I., Butler, T., Co-

fala, J., Collins, W. J., Derwent, R. G., Doherty, R. M., Drevet, J., Eskes, H. J., Fiore, A. M., Gauss, M., Hauglustaine, D. A., Horowitz, L. W., Isaksen, I. S. A., Krol, M. C., Lamarque, J. F., Lawrence, M. G., Montanaro, V., Müller, J. F., Pitari, G., Prather, M. J., Pyle, J. A., Rast, S., Rodriquez, J. M., Sanderson, M. G., Savage, N. H., Shindell, D. T., Strahan, S. E., Sudo, K., and Szopa, S.: Multimodel ensemble simulations of present-day and near-future tropospheric ozone, J. Geophys. Res.-Atmos., 111, D08301, doi:10.1029/2005JD006338, 2006.
Stohl, A., Bonasoni, P., Cristofanelli, P., Collins, W., Feichter, J., Frank, A., Forster, C., Gerasopoulos, E., Gäggeler, H., James, P., Kentarchos, T., Kromp-Kolb, H., Krüger, B., Land, C., Meloen, J., Papayannis, A., Priller, A., Seibert, P., Sprenger, M., Roelofs, G. J., Scheel, H. E., Schnabel, C., Siegmund, P., Tobler, L., Trickl, T., Wernli, H., Wirth, V., Zanis, P., and Zerefos, C.: Stratosphere–troposphere exchange: a review, and what we have learned from STACCATO, J. Geophys. Res.-Atmos., 108, 8516, doi:10.1029/2002JD002490, 2003.
Talbot, R., Mao, H., and Sive, B.: Diurnal characteristics of surface level O_3 and other important trace gases in New England, J. Geophys. Res.-Atmos., 110, 1–16, doi:10.1029/2004JD005449, 2005.
Thompson, D. W. J. and Wallace, J. M.: The Arctic oscillation signature in the wintertime geopotential height and temperature fields, Geophys. Res. Lett., 25, 1297, doi:10.1029/98GL00950, 1998.
Thompson, D. W. J. and Wallace, J. M.: Annular mode in the extratropical circulation. Part I: Month-to-month variability, J. Climate, 13, 1000–1016, 2000.
Tilmes, S., Lamarque, J.-F., Emmons, L. K., Conley, A., Schultz, M. G., Saunois, M., Thouret, V., Thompson, A. M., Oltmans, S. J., Johnson, B., and Tarasick, D.: Technical Note: Ozonesonde climatology between 1995 and 2011: description, evaluation and applications, Atmos. Chem. Phys., 12, 7475–7497, doi:10.5194/acp-12-7475-2012, 2012.
Tohjima, Y., Kubo, M., Minejima, C., Mukai, H., Tanimoto, H., Ganshin, A., Maksyutov, S., Katsumata, K., Machida, T., and Kita, K.: Temporal changes in the emissions of CH_4 and CO from China estimated from CH_4 / CO_2 and CO / CO_2 correlations observed at Hateruma Island, Atmos. Chem. Phys., 14, 1663–1677, doi:10.5194/acp-14-1663-2014, 2014.
U.S. Environmental Protection Agency (EPA): Our Nation's Air Status and Trends Through 2010, available at: http://www3.epa.gov/airtrends/2011/, 2012.
U.S. Environmental Protection Agency (EPA): National Ambient Air Quality Standards for Ozone; Proposed Rule, Fed. Regist., 79, 75234, doi:10.2753/RSH1061-1983310140, 2014.

West, J. J., Fiore, A. M., Horowitz, L. W., and Mauzerall, D. L.: Global health benefits of mitigating ozone pollution with methane emission controls, P. Natl. Acad. Sci. USA, 103, 3988–3993, doi:10.1073/pnas.0600201103, 2006.

Wigder, N. L., Jaffe, D. A., and Saketa, F. A.: Ozone and particulate matter enhancements from regional wildfires observed at Mount Bachelor during 2004–2011, Atmos. Environ., 75, 24–31, doi:10.1016/j.atmosenv.2013.04.026, 2013.

Wild, O. and Akimoto, H.: Intercontinental transport of ozone and its precursors in a three-dimensional global CTM, J. Geophys. Res.-Atmos., 106, 27729–27744, doi:10.1029/2000JD000123, 2001.

Wilson, R. C., Fleming, Z. L., Monks, P. S., Clain, G., Henne, S., Konovalov, I. B., Szopa, S., and Menut, L.: Have primary emission reduction measures reduced ozone across Europe? An analysis of European rural background ozone trends 1996–2005, Atmos. Chem. Phys., 12, 437–454, doi:10.5194/acp-12-437-2012, 2012.

Woollings, T. and Blackburn, M.: The north Atlantic jet stream under climate change and its relation to the NAO and EA patterns, J. Climate, 25, 886–902, doi:10.1175/JCLI-D-11-00087.1, 2012.

Worden, H. M., Deeter, M. N., Frankenberg, C., George, M., Nichitiu, F., Worden, J., Aben, I., Bowman, K. W., Clerbaux, C., Coheur, P. F., de Laat, A. T. J., Detweiler, R., Drummond, J. R., Edwards, D. P., Gille, J. C., Hurtmans, D., Luo, M., Martínez-Alonso, S., Massie, S., Pfister, G., and Warner, J. X.: Decadal record of satellite carbon monoxide observations, Atmos. Chem. Phys., 13, 837–850, doi:10.5194/acp-13-837-2013, 2013.

World Meteorological Organization: WMO Greenhouse Gas Bulletin: The State of Greenhouse Gases in the Atmosphere Based on Global Observations through 2011, No 8, 4, 2012.

Wotawa, G. and Trainer, M.: The influence of Canadian forest fires on pollutant concentrations in the United States, Science, 288, 324–328, doi:10.1126/science.288.5464.324, 2000.

Wotawa, G., Novelli, P. C., Trainer, M., and Granier, C.: Inter-annual variability of summertime CO concentrations in the Northern Hemisphere explained by boreal forest fires in North America and Russia, Geophys. Res. Lett., 28, 4575–4578, doi:10.1029/2001GL013686, 2001.

Xing, J., Pleim, J., Mathur, R., Pouliot, G., Hogrefe, C., Gan, C.-M., and Wei, C.: Historical gaseous and primary aerosol emissions in the United States from 1990 to 2010, Atmos. Chem. Phys., 13, 7531–7549, doi:10.5194/acp-13-7531-2013, 2013.

Xing, J., Mathur, R., Pleim, J., Hogrefe, C., Gan, C.-M., Wong, D. C., Wei, C., Gilliam, R., and Pouliot, G.: Observations and modeling of air quality trends over 1990–2010 across the Northern Hemisphere: China, the United States and Europe, Atmos. Chem. Phys., 15, 2723–2747, doi:10.5194/acp-15-2723-2015, 2015.

Xu, X., Lin, W., Wang, T., Yan, P., Tang, J., Meng, Z., and Wang, Y.: Long-term trend of surface ozone at a regional background station in eastern China 1991–2006: enhanced variability, Atmos. Chem. Phys., 8, 2595–2607, doi:10.5194/acp-8-2595-2008, 2008.

Zhang, Q., Streets, D. G., Carmichael, G. R., He, K. B., Huo, H., Kannari, A., Klimont, Z., Park, I. S., Reddy, S., Fu, J. S., Chen, D., Duan, L., Lei, Y., Wang, L. T., and Yao, Z. L.: Asian emissions in 2006 for the NASA INTEX-B mission, Atmos. Chem. Phys., 9, 5131–5153, doi:10.5194/acp-9-5131-2009, 2009.

Zhou, X., Huang, G., Civerolo, K., Roychowdhury, U., and Demerjian, K. L.: Summertime observations of HONO, HCHO, and O_3 at the summit of Whiteface Mountain, New York, J. Geophys. Res.-Atmos., 112, 1–13, doi:10.1029/2006JD007256, 2007.

Table 1. Ground stations with geographical coordinates and measurement periods.

Site	Latitude	Longitude	Elevation	Measurement Period (CO)	Measurement Period (O_3)
Appledore Island (AI)	42.97° N	70.62° W	18 m	Jul 2001–Jul 2011	Jul 2002–Mar 2012
Thompson Farm (TF)	43.11° N	70.95° W	23 m	Apr 2001–Jul 2011	Apr 2001–Aug 2010
Mt. Washington (MWO)	44.27° N	71.30° W	1917 m	Apr 2001–Apr 2009	Apr 2001–May 2010
Castle Spring (CS)	43.75° N	71.35° W	396 m	Apr 2001–Jun 2008	Apr 2001–May 2008
Pack Monadnock (PM)	42.86° N	71.88° W	698 m	Jun 2004–Jul 2011	Jul 2004–Oct 2008
Whiteface Mountain (WFM)	44.40° N	73.90° W	1484 m	Jan 1996–Dec 2010	Jan 1996–Dec 2010
Pinnacle State Park (PSP)	42.09° N	77.21° W	504 m	Jan 1997–Dec 2010	Jan 1997–Dec 2010

Note: CO and O_3 at AI were measured seasonally from May to September before 2007/08. Year-round measurements of CO and O_3 began in May 2007 and February 2008, respectively.

Table 2. Trends (ppbv yr^{-1}) of baseline CO and O_3 in spring, summer, fall, and winter.

Site	Period	Spring CO	Spring O_3	Summer CO	Summer O_3	Fall CO	Fall O_3	Winter CO	Winter O_3	Annual CO	Annual O_3
AI	2002–2010			0.8(0.66)	**−3.1(0.07)**						
CS	2001–2008	3.4 (0.06)	0.9 (0.65)	2.4 (0.19)	−2.9 (0.14)	1.1 (0.57)	1.5 (0.45)	6.1 (< 0.01)	0.4 (0.86)	**2.8 (< 0.01)**	0.8 (0.39)
MWO	2001–2009	−13.2 (0.51)	−0.7 (0.71)	**−4.5 (0.01)**	**−4.7 (0.01)**	**−4.4 (0.01)**	−0.9 (0.64)	−1.7 (0.36)	0.1 (0.98)	**2.3 (< 0.01)**	0.7 (0.42)
PM	2005–2010	**−6.5 (< 0.01)**	−1.9 (0.39)	**−5.5 (< 0.01)**	−3.5 (0.14)	**−4.2 (0.05)**	−3.4 (0.11)	**−5.5 (0.01)**	0.1 (1.00)	**3.5 (< 0.01)**	0.8 (0.43)
TF	2001–2010	**−3.7 (0.02)**	**2.4 (0.10)**	**−4.5 (< 0.01)**	−0.1 (0.94)	**−3.2 (0.04)**	0.2 (0.90)	**−4.8 (< 0.01)**	**2.7 (0.09)**	**2.5 (< 0.01)**	0.8 (0.29)
PSP	2001–2010	**−4.5 (< 0.01)**	1.3 (0.43)	**−4.3 (< 0.01)**	−0.8 (0.57)	**−4.2 (0.01)**	−1.9 (0.23)	**−3.9 (0.02)**	−0.7 (0.68)	**4.3 (< 0.01)**	0.7 (0.40)
WFM	2001–2010	−0.5 (0.78)	0.4 (0.83)	−1.9 (0.23)	**−4.7 (< 0.01)**	**−6.4 (< 0.01)**	0.5 (0.76)	−2.1 (0.21)	−1.3 (0.45)	**2.8 (< 0.01)**	0.9 (0.27)

p values are in the parentheses.
Boldfaced numbers indicate *p* value < 0.10.

Table 3. The contributions, in R^2, of CO emissions from wildfires over Russia, Canada, Alaska, and California to variation in baseline CO at each site. The combined effect of wildfire emissions over Russia and Canada was also computed.

	Russia		Canada		Alaska		California		Combined	
	R^2	p	R^2	p	R^2	p	R^2	p	R^2	p
AI	**0.39**	**0.01**	0.12	0.15	0.13	0.19	0.12	0.21	**0.41**	**0.02**
CS	**0.41**	**0.01**	**0.17**	**0.09**	0.06	0.38	< 0.01	0.92	**0.41**	**0.02**
MWO	**0.41**	**0.01**	0.13	0.15	0.01	0.77	< 0.01	0.88	**0.43**	**0.02**
TF	**0.64**	**0.01**	**0.40**	**0.05**	0.01	0.80	0.03	0.52	**0.65**	**0.01**
PSP	0.11	0.18	0.15	0.11	0.09	0.27	< 0.01	0.93	0.16	0.27
WFM	**0.32**	**0.01**	**0.32**	**0.01**	< 0.01	0.90	0.01	0.69	**0.38**	**0.03**
Mean	0.38		0.22		< 0.05		< 0.03		0.41	

Note: PM was not included due to insufficient data.
Boldfaced numbers indicate p value < 0.10.

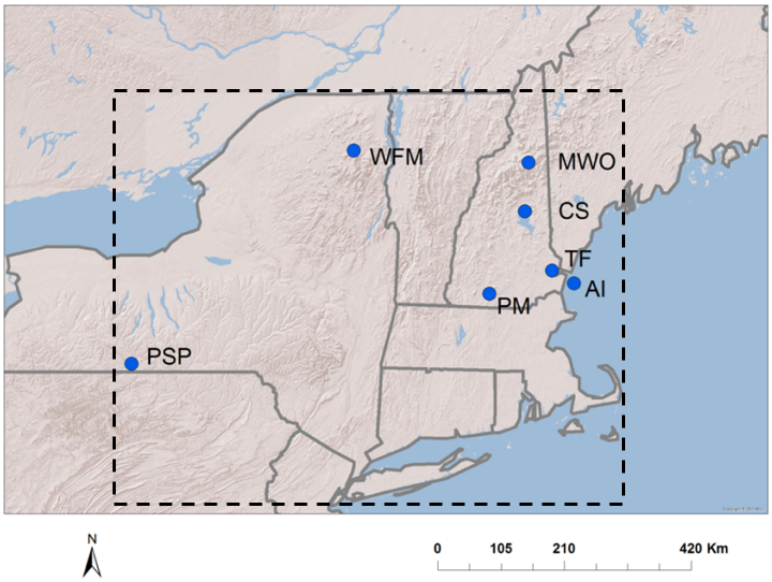

Figure 1. Map of the northeast US. The seven measurement sites used in the study are marked with blue dots.

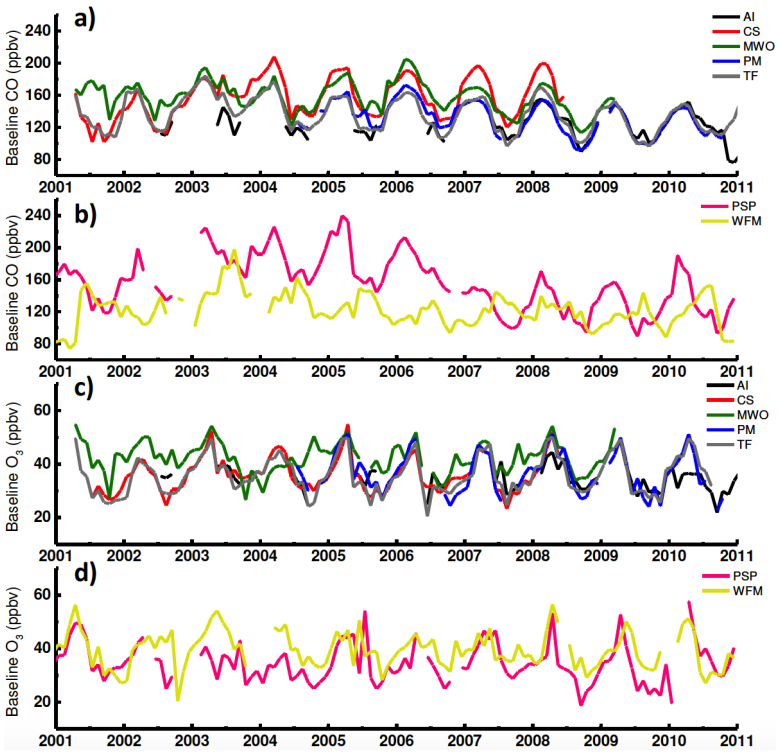

Figure 2. Monthly baseline CO (ppbv) at **(a)** AI, CS, MWO, PM, and TF, and **(b)** MWO and PSP. Monthly baseline O_3 (ppbv) at **(c)** AI, CS, MWO, PM, and TF, and **(d)** MWO and PSP.

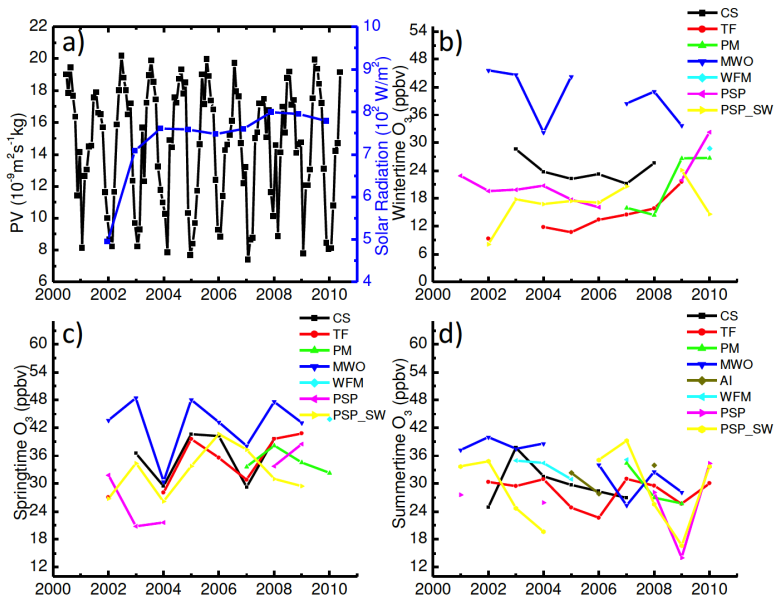

Figure 3. (a) Time series of monthly PV (10^{-9} m^2 s^{-1} kg) at 350 K over the study region (40–45° N, 70–77.5° W, indicated with dashed box in Fig. 1) and averaged daily maximum solar radiation flux at TF in spring (March–May). Seasonal 10th percentile mixing ratios of O_3 with wind from the directions aligned with the urban corridor in **(b)** winter, **(c)** spring, and **(d)** summer. Specifically, the wind directions selected for AI: 157.5–202.5°; CS: 157.5–202.5°; MWO: 157.5–202.5°; PM: 112.5–157.5°; TF: 157.5–202.5°; WFM: 112.5–157.5°; PSP: 67.5–112.5°. In addition, seasonal 10th percentile mixing ratios of O_3 at PSP with wind from the directions aligned with the Ohio River Valley was calculate as PSP_SW (202.5–247.5 °) in **(b)**, **(c)**, and **(d)**.

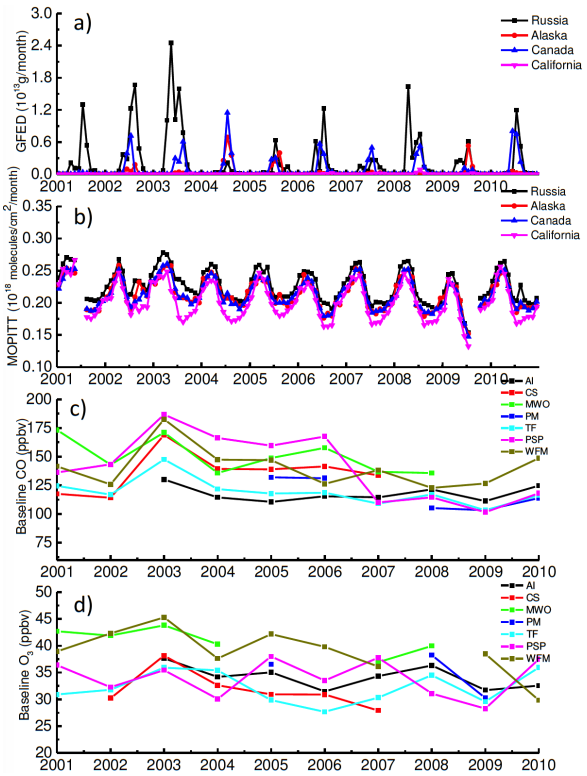

Figure 4. (a) CO emissions from biomass burning based on GFED dataset. **(b)** Total CO columns based on MOPITT retrievals over Russia (black), Alaska (red), Canada (blue), and California (magenta). Summertime averaged baseline **(c)** CO and **(d)** O_3 at each site.

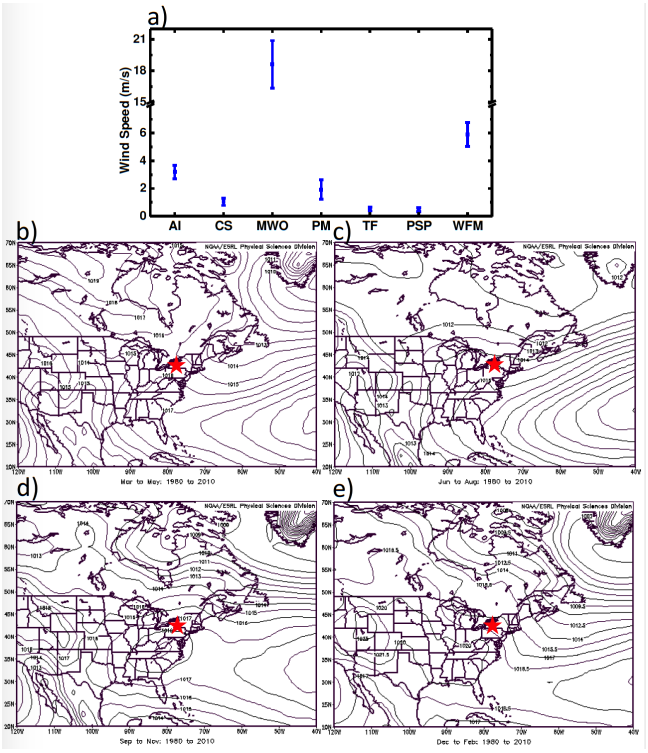

Figure 5. (a) Annual surface wind speed with yearly variation at each site over summer 2001–2010. northeast US sea surface pressure (hPa) in **(b)** spring, **(c)** summer, **(d)** fall, and **(e)** winter. Red stars indicate the location of PSP.

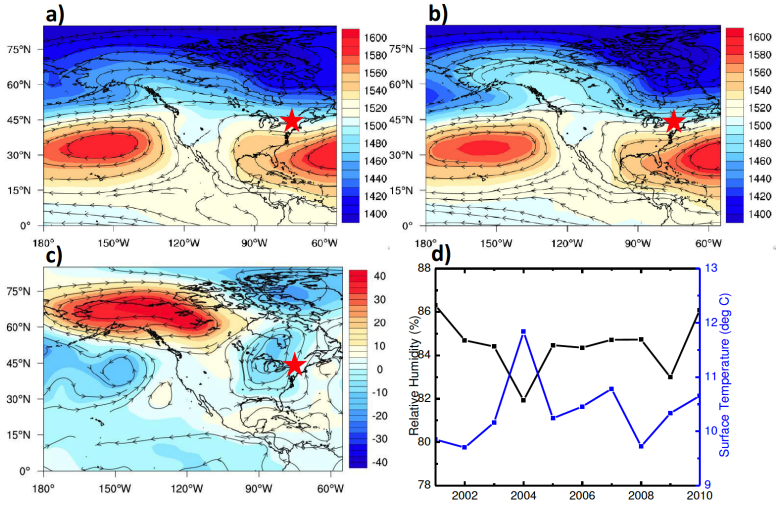

Figure 6. Geopotential height at the 850 hPa pressure level during summer in **(a)** 2001–2010 **(b)** 2004. **(c)** The difference of geopotential height at 850 hPa between summer 2004 and the 10-year average. **(d)** The annual surface temperature and relative humidity over Alaska and southwestern Canada (55–70° N, 110–160° W) over summer 2001–2010. Red stars indicated the area of the study sites. (Source: NCEP/NCAR reanalysis)

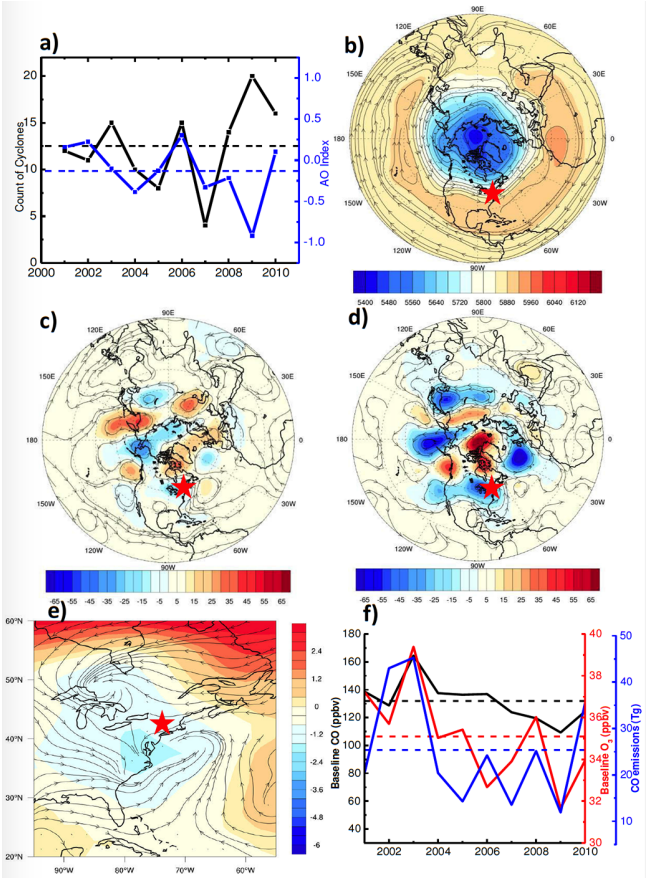

Figure 7. (a) Counts of cyclones in the northeast US (black) and the AO index (blue) in summer. **(b)** Geopotential height at 500 hPa from the NCEP/NCAR reanalysis data during summer 2001–2010. **(c)** The difference of geopotential height at 500 hPa between years with strong (2003, 2006, 2008, 2009, and 2010) and weak (2001, 2002, 2004, 2005, and 2007) cyclone activities. **(d)** The difference of geopotential height at 500 hPa between summer 2009 and the 10-year means. **(e)** The difference of sea level pressure between summer 2009 and the 10-year means. **(f)** Time series of summertime baseline CO (black) and baseline O_3 (red) averaged over all sevent sites, and Time series of CO emissions (blue) from wildfires in Russia and Canada. Dashlines indicate the 10-year means. Red stars indicate the area of the study sites.

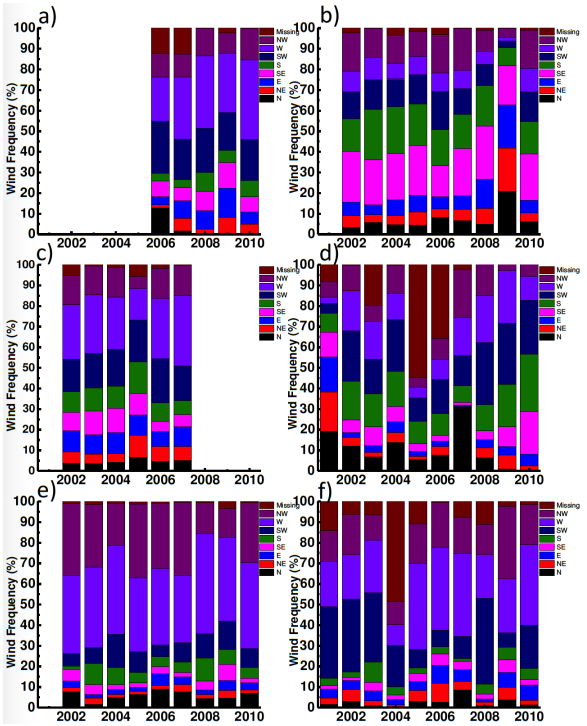

Figure 8. Wind frequency in summer at **(a)** PM, **(b)** MWO, **(c)** CS, **(d)** WFM, **(e)** TF, **(f)** PSP. N: −22.5–22.5°; NE: 22.5–67.5°; E: 67.5–112.5°; SE: 112.5–157.5° ; S: 157.5–202.5°; SW: 202.5–247.5°; W: 247.5–337.5°; NW: 337.5° to −22.5°.

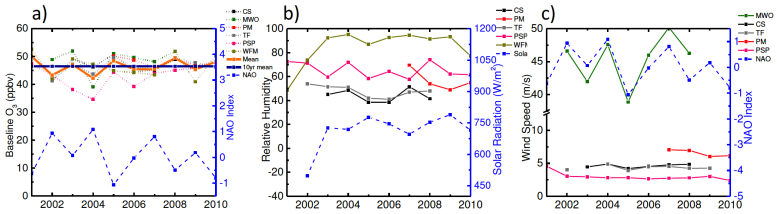

Figure 9. (a) Baseline O_3 and the NAO index averaged in March and April. The thick orange line indicates the baseline O_3 averaged over the seven sites and the thick dark blue line indicates the mean value 46.5 ppbv over 2001–2010. **(b)** Averaged daytime (18:00–24:00 UT) relative humidity and daily maximum solar radiation flux at TF in March and April. **(c)** Averaged wind speed ($> 2\,m\,s^{-1}$) from the west (247.5–337.5°) and the NAO index in March and April.

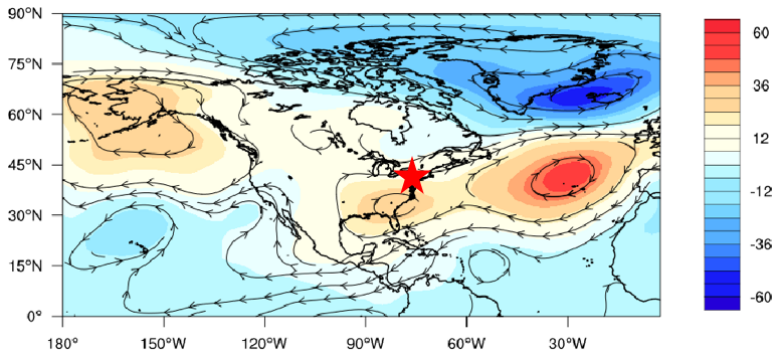

Figure 10. The difference of geopotential height (m) and streamlines at 850 hPa between the low O_3 years (2002, 2004, 2006, 2007, and 2009) and high O_3 years (2001, 2003, 2005, 2008, and 2010). The red star indicates the area including the study sites.

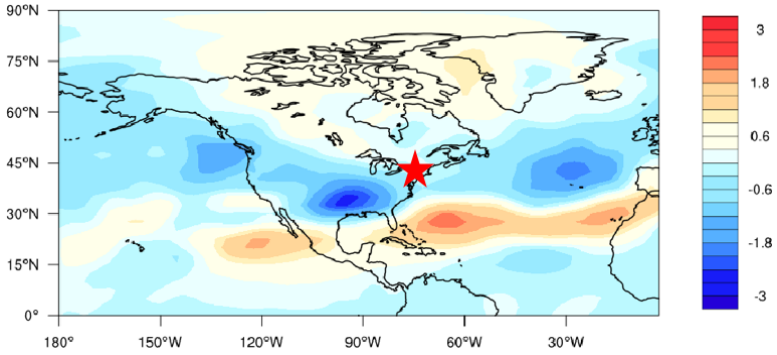

Figure 11. Same as Fig. 10 except that the difference of PV (10^{-9} m^2 s^{-1} kg) at 350 K is shown.